CHALMERS
UNIVERSITY OF TECHNOLOGY

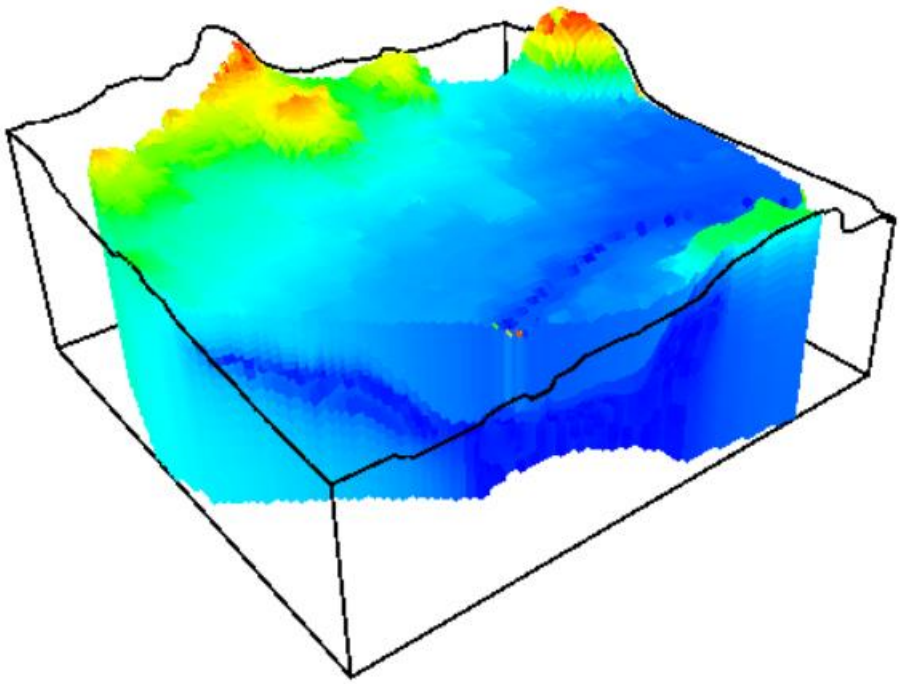

Towards Benchmarking Time Series Analysis with Process-Based Groundwater Models

The Case of Hydrogeological Impacts of Tunnel Construction

Master's Thesis in Infrastructure and Environmental Engineering

ERIK LILJA
ZACKARIAS ZANDER

DEPARTMENT OF Architecture and Civil Engineering
CHALMERS UNIVERSITY OF TECHNOLOGY
Gothenburg, Sweden 2024
www.chalmers.se

MASTER'S THESIS 2024

Towards Benchmarking Time Series Analysis with Process-Based Groundwater Models

The Case of Hydrogeological Impacts of Tunnel Construction

ERIK LILJA
ZACKARIAS ZANDER

CHALMERS
UNIVERSITY OF TECHNOLOGY

Department of Architecture and Civil Engineering
Geology and Geotechnics
CHALERS UNIVERSITY OF TECHNOLOGY
Gothenburg, Sweden 2024

Towards Benchmarking Time Series Analysis with Process-Based Groundwater Models
The Case of Hydrogeological Impacts of Tunnel Construction

ERIK LILJA
ZACKARIAS ZANDER

Supervisor: Ezra Haaf, Architecture and Civil Engineering, Chalmers University of Technology
Supervisor: Stefan von Wachenfeldt Falemo, Hydrogeology and Geophysics, AFRY
Examiner: Lars Rosen, Architecture and Civil Engineering, Chalmers University of Technology

Master's Thesis 2024
Department of Architecture and Civil Engineering
Division of Geology and Geotechnics
Chalmers University of Technology
SE-412 96 Gothenburg
Telephone +46 31 772 1000

Cover: 3D view of the MODFLOW model

Gothenburg, Sweden 2024

Towards Benchmarking Time Series Analysis with Process-Based Groundwater Models
The Case of Hydrogeological Impacts of Tunnel Construction

ERIK LILJA
ZACKARIAS ZANDER
Department of Architecture and Civil Engineering
Chalmers University of Technology

Abstract

This thesis evaluates time series modelling for investigating groundwater impacts due to tunnelling in an urban environment based on a process-based, benchmark groundwater model. The Haga site in Gothenburg, Sweden, as part of the Västlänken infrastructure project was used as case study area.

Utilizing datasets from various sources, including climate data from SMHI, head observations from the Haga site, and MODFLOW simulations. The study employs MODFLOW simulations and time series analysis to simulate and evaluate GW dynamics. Through Python-based transfer function noise modelling (TFN) using the Pastas package, the study constructs time series models to assess potential tunnel leakage and its impact on GW levels. The thesis emphasizes the importance of accurate data collection and precise modelling techniques to correctly calibrate the model to show the effects on GW systems.

The calibration of the MODFLOW model showed good correlation with observed groundwater data, but urban complexities and model limitations caused discrepancies. Refinements, such as improved calibration techniques and improving the representation of groundwater recharge, could enhance model accuracy. The TFN models demonstrated strong performance, especially with added stress data of tunnel leakage. This indicates that the ability of TFN models to investigate groundwater impacts can be benchmarked with a groundwater flow model. However, this study also highlighted challenges due to data scarcity, leading to mismatches between groundwater observations and simulations with the benchmark model, which in future studies could be addressed with more advanced calibration and integration techniques. Future research should focus on refining these models and investigating the skill of TFN models when more groundwater impacts are present.

Keywords: Transfer function-noise modelling, Time series analysis, Pastas, MODFLOW model, groundwater.

Acknowledgements

This thesis work, conducted during the spring of 2024, marks the culmination of the master's programme in Infrastructure and Environmental Engineering. The inception of this project stemmed from insightful discussions with our supervisors at AFRY and Chalmers, specifically Stefan von Wachenfeldt Falemo and Ezra Haaf. Their invaluable guidance and support were instrumental in shaping the trajectory of our research. We extend our sincere gratitude to them for their unwavering assistance throughout the project.

Furthermore, we would like to express our appreciation to the individuals at the Department of Hydrogeology at AFRY for providing us with a conducive environment for our work and helping whenever needed. Special thanks also go to Jonas Sundell at SGI for his expertise and support in understanding the MODFLOW model.

This project would not have been possible without the collaborative efforts and support of these individuals, and we are truly grateful for their contributions.

Erik Lilja & Zackarias Zander, Gothenburg, May 2024

List of Acronyms

EPA	Environmental protection agency
GUI	Graphical User Interface
SGU	Swedish Geological Survey (Sveriges Geologiska Undersökning)
SMHI	Swedish Meteorological and Hydrological Institute
TFN	Transfer Function Noise

Glossary

Aquifer	A body of permeable rock or soil layer that can contain or transmit GW.
Basev Moraine	A type of till deposited at the base of a glacier, typically containing a mix of clay, sand, and gravel.
Finite Difference Method	A numerical technique used to approximate solutions to differential equations, applied in MODFLOW for GW modelling.
Calibration	The process of adjusting model parameters to match observed data.
Confining Layer	A layer of low permeability that restricts the flow of GW.
GW Head	The level of water in an aquifer, typically measured in meters above a reference point.
Infiltration	Refers to the movement of water from the surface into the soil, which is crucial for GW recharge and reducing surface runoff.
Influence Area	The area affected by changes in GW flow or head due to a particular feature or activity, such as a tunnel.
ModelMuse	A graphical user interface (GUI) used to create and manage MODFLOW GW models.
MODFLOW	A widely used GW modelling software developed by the US Geological Survey, employing the finite difference method to simulate GW flow.
MODFLOW NWT	A variant of MODFLOW-2005 based on the Newton Raphson formulation that offers enhanced capabilities for simulating complex GW systems, particularly useful in scenarios with unconfined aquifers.
Pastas	A Python-based package for time series analysis in hydrology, used for modelling GW levels and flows.
PyEt	A Python-based package for calculating Potential Evapotranspiration, (PET)
R^2 (R-squared)	Coefficient of Determination, a statistical measure of how well the observed outcomes is replicated by the model.
r_s	Spearman's correlation coefficient, a statistical measure of the relationship between two sets of data.
Recharge	Describes the replenishment of GW resources through the infiltration of water, mainly from precipitation, into aquifers.
Swedish Environmental Code (Miljöbalken)	The primary legal instrument for environmental protection in Sweden, focusing on sustainable use of natural resources and preserving ecosystems.
Swedish Transport Administration (Trafikverket)	The authority responsible for planning, developing, and maintaining Sweden's transportation infrastructure to ensure it is safe, efficient, and sustainable.

Contents

List of Figures

List of Tables

List of Appendices

1
Introduction

The lowering of groundwater head due to anthropogenic activities like tunnel construction can lead to consequences such as settlements that can have significant impacts on nearby structures (Yoo, 2016). This occurs because as the groundwater head declines, the soil loses strength (Shen & Xu, 2006). In urban areas, the process of groundwater formation differs due to the presence of impervious surfaces like paved areas and buildings, which reduce opportunities for infiltration and increase runoff (Markovič, et.al., 2014).

Leakage to tunnels has always been troublesome, and the effect on the surrounding environment has received increasing attention in recent years (Spross, 2009). As the leakage may cause lowering of groundwater levels. The conductivity of the surrounding rock governs the amount of water that can flow into the tunnel, and this can be controlled by e.g. grouting to increase conductivity and reduce groundwater leakage (Florén, 2015).

Activities with the potential to affect water resources are regulated by the Swedish environmental code, requiring authorization from the Environmental Court (Spross, 2009). This authorization is needed early in projects, often before work can begin on-site, and it controls the size of protective measures required.

Making precise calculations from the start can help optimize protective measures such as tunnel grouting (Vägverket, 2000). This optimization can lead to environmental benefits by reducing carbon emissions associated with cement-based grout production and economic benefits by minimizing unnecessary costs associated with overestimated grouting needs in tunnelling projects (Sundell, et.al., 2019).

Using a numerical groundwater model can be a valuable tool for groundwater management. However, due to data limitations, particularly at the early stages of an infrastructure project, the process of setting up a numerical model can be challenging. Insufficient data and low-resolution data can lead to difficulties in forecasting changes in e.g. groundwater head accurately (Haaf, et.al., 2023). In contrast, a time series model can be advantageous as it requires a sparser set of data. A time series model can rely on historical GW measurements and does not need as many inputs regarding site characteristics (Collenteur, 2019). It can be both faster to set up and more user-friendly compared to a numerical model (Bakker, 2019).

Impulse response functions (IRFs) are essential tools in groundwater modeling, particularly within the framework of Transfer Function-Noise (TFN) modeling (Lu, et.al., 2022). IRFs characterize the response of a system to a unit impulse of stress, enabling a detailed understanding of how various stresses affect the system over time. By superimposing stress models, which involves summing the effects of individual stresses, it is possible to identify and quantify the contributions of different stresses to the observed system behavior.

In the context of TFN modeling, the primary objective is to relate observed time series data, such as groundwater levels, to a set of input stresses, including precipitation, pumping, leakage (Pezij, et.al., 2020). This is achieved by developing transfer functions for each stress, which mathematically describe the system's response to a unit change in that stress. The noise component in TFN models accounts for unexplained variability and model residuals, ensuring a more accurate and realistic representation of the system.

Despite their benefits, the level to which time series models can be used for identifying groundwater impacts from subsurface construction have not yet been sufficiently tested. Conducting experiments and research in urban areas can be problematic due to various uncertainties that complicate time series modelling. To evaluate time series models in different areas with limited field data, synthetic time series can be created based on a process-based numerical model (Vonk et. al., 2024). This model can then be used as a benchmark model that generates simulated time series based on different scenarios for evaluation with time series models.

In this thesis, a benchmark model is created to simulate time series in an urban environment in the context of a tunnel project. The benchmark model was developed using MODFLOW to simulate the GW levels at the Haga site in Gothenburg, which is part of the Västlänken railway project. The simulated time series were used as synthetic time series for a time series model using Impulse-Response function as implemented in the Python package Pastas 1.5.0.

1.1 Aim

The aim of this thesis is to assess the feasibility of using a numerical model as a basis for benchmarking TFNs to estimate the effects of tunnel construction on groundwater head. This involves running a scenario of impacted groundwater head due to tunnel construction in a numerical groundwater flow model, generating simulated head observation time series, which are subsequently modelled with TFN. By comparing the outputs of these different models, the study aims to determine the correlation between the results, thereby providing insights into the accuracy and reliability of the time series model.

1.2 Research questions

The research questions proposed for this paper are:

- How can a MODFLOW model that simulates groundwater leakage to a tunnel be calibrated for use as a benchmark model for time series analysis?
- Can simulated time series from a benchmark model be used to create a representative Time series model for estimation of the effect of leakage?

1.3 Limitations

Based on the analysis which are to be performed there are certain limitations due to the chosen study area and proposed modelling methodology. To conclude this chapter the most relevant limitations are presented in the list below.

- Limited data availability for certain wells, and this means that the analysis performed was limited to wells with enough data present.
- Limited data availability regarding measured infiltration data is not available meaning the TFN model accuracy may be limited.
- Adding a tunnel in the benchmark model may not capture the intricacies of adding a real tunnel and may too much of an oversimplification.

2
Study Area

The chosen study area is Haga in Gothenburg, Sweden, which is currently undergoing the Västlänken infrastructure project involving the construction of a tunnel beneath Gothenburg. Data from both preliminary studies and ongoing work on the project are accessible. Additionally, a calibrated MODFLOW model for Haga had been developed by Pool et.al. (2024), further justifying the selection of this site.

2.1 Västlänken, Haga site

Västlänken is a commuter train tunnel being built underneath Gothenburg, Sweden aimed at enhancing railway capacity (Trafikverket, 2013). The Haga area, in central Gothenburg is integral to Västlänken and involves the construction of 1700 meters of tunnel, as well as a commuter train tunnel passing through both soil and bedrock (Trafikverket, 2022). In Figure 1, the Haga site is highlighted in red within the overview of the Västlänken project.

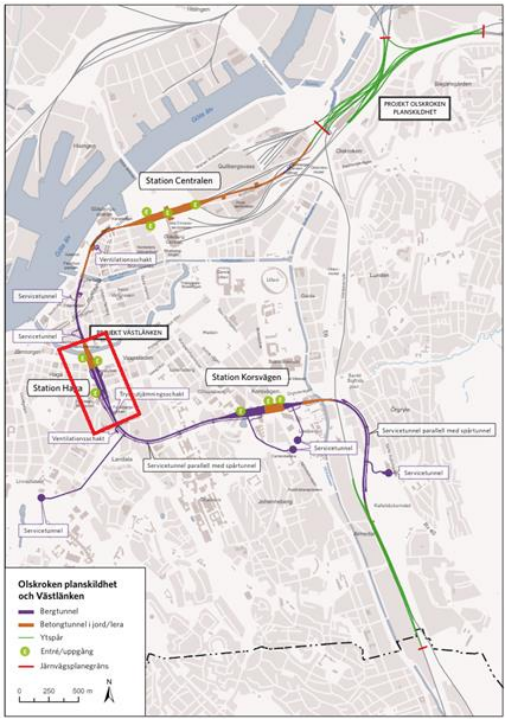

Figure 1 Overview of the project Västlänken in Gothenburg (Trafikverket, 2015).

The Haga tunnel primarily crosses through bedrock, comprising 1450 meters of bedrock tunnel and 250 meters of tunnel in soil (Trafikverket, 2022). Figure 2 provides a visualization of the Västlänken tunnel project, with the Haga site delineated in red. The geological composition of the area includes filling material, clay, gravel, and bedrock, arranged in layers from top to bottom (Trafikverket, 2020).

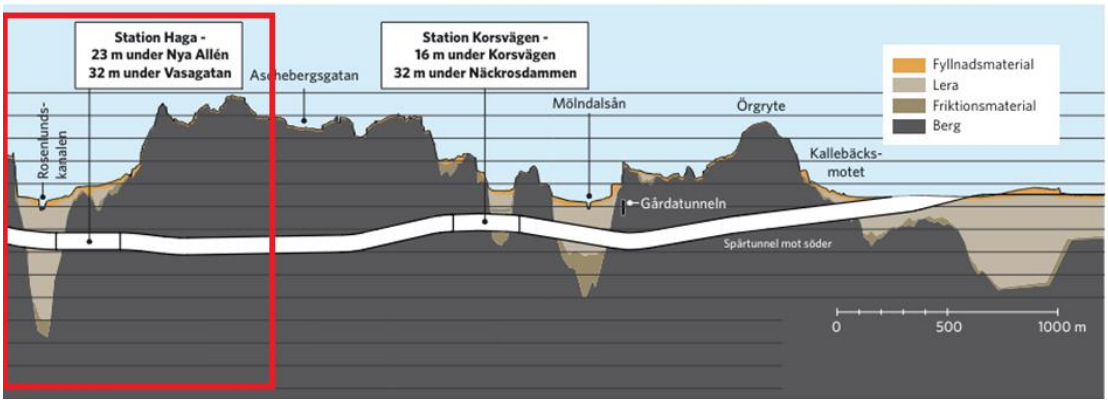

Figure 2 Visualization of the tunnel for Västlänken (Trafikverket, 2020) Haga site are marked in red.

2.1.1 Geology

In Sweden, the bedrock primarily comprises Precambrian crystalline rocks, with some regions featuring younger sedimentary rock formations (SGU, 2020a). Figure 3, illustrates that the study area in Haga is predominantly composed of Tonalite-Granodiorite, an igneous intrusive rock, seen as the beige area in the figure. These rocks originate from the Sveconorwegian orogeny, dating back approximately 1.66-1.59 billion years. Additionally, Figure 3 highlights the presence of a deformation zone, indicated by the black dashed line, which traverses parts of the proposed tunnel location, seen as the highlighted area. This geological feature has the potential to increase leakage into the tunnel, as fracture zones may serve as conduits for water flow (Florén, 2015).

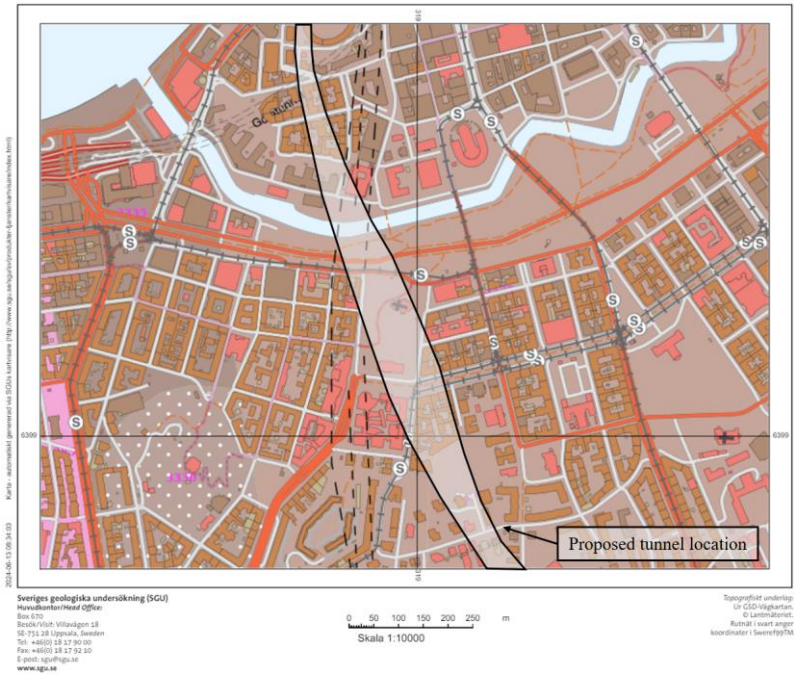

Figure 3 Bedrock map from SGU (2023).

2.1.2 Hydrogeology

The soil stratigraphy, depicted in Figure 4, provides valuable insights. Layers 1 and 2, represented in the topmost part, consist of filling material, likely a combination of sand and coarser-grained materials like gravel. Historically, Gothenburg was located below the highest coastline before and after the last ice age, experiencing both transgressions and regressions due to isostatic adjustments (SGU, 2020b). Therefore, the clay present at the site is a combination of glacial and post-glacial clay. The yellow section corresponds to this clay, which impacts the site's hydraulics due to its variable hydraulic conductivity. Despite its variability, clay serves as a confining layer for the underlying coarse-grained material, which forms the confined aquifer in the lower section (USGS, 2003).

The confined aquifer likely consists of till, specifically ground moraine characterized by the presence of clay and sand (USGS, 2020) The layer beneath, labelled as "top bedrock" in Figure 4, consists of weathered bedrock. This weathered bedrock was formed due to the movement and weight of ice sheets across the landscape, making this section more permeable due to the resulting deformations (SGU, 2020c). The section of bedrock not affected by the weathering process is labelled as "bedrock" in Figure 4.

The soil type for the confined aquifer consists of coarser-grained material, giving it hydraulic properties conducive to water-bearing, thereby forming an aquifer (USGS, n.d). The weathered bedrock has a higher propensity to exhibit fractures, which can transport water. The water-bearing capacity of these fractures depends on the rock type (Fischer, et.al., 2022). The bedrock falls into the category of crystalline rock, which often exhibits complex fracture structures characterized by long fractures forming intricate 3-dimensional systems (Florén, 2015).

The potential for complex, spatially spread fractures makes estimating groundwater formation and groundwater head levels increasingly difficult in areas with weathered bedrock consisting of crystalline rock (Florén, 2015). The bottommost layer of the area is the unweathered part of the bedrock, consisting of a mostly continuous body of matter. This layer does not exhibit fractures to the same extent, as the probability of finding fractures diminishes with depth due to the decreasing stresses on the rock (Florén, 2015).

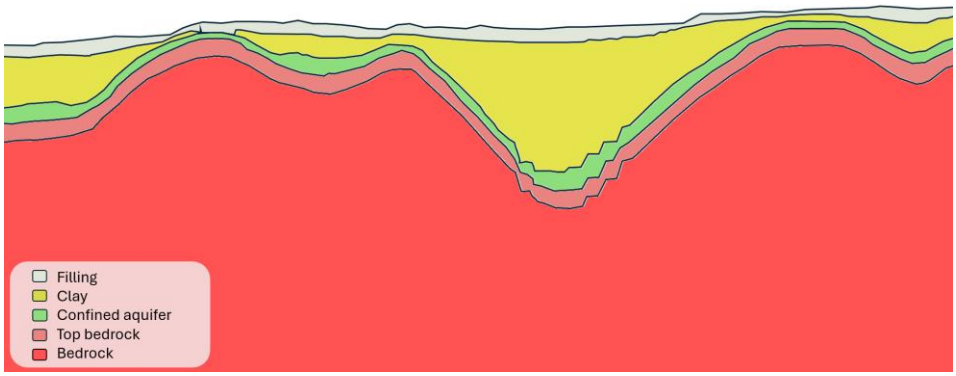

Figure 4 Depiction of the soil stratigraphy for a section of the Haga area derived from ModelMuse.

2.2 MODFLOW Model

The numerical model utilized in this thesis was built and pre-calibrated based on pumping tests conducted in the area during 2019 (Pool, et.al., 2024). The boundary condition used in the base configuration was set to a constant head boundary condition, however the boundary condition may be changed to reflect other scenarios.

The MODFLOW model utilized in this thesis is implemented using ModelMuse, an open-source graphical user interface (GUI) that allows efficient processing of input data to MODFLOW (USGS, 2021). MODFLOW, a finite difference method, is widely used for groundwater modelling, with several variants available (USGS, 2022a). The specific variant employed in this model is MODFLOW NWT, which is a modified version of MODFLOW-2005. One notable advantage of using MODFLOW NWT is its enhanced flexibility in adjusting model parameters and rewetting implementation. (USGS, 2022b). Rewetting allows for cells which have been dried out and thus becoming inactive to be reactivated as the water table rises. In Figure 5, a snapshot of the Haga model area in ModelMuse illustrates the visualization of the model setup.

Figure 5: Snapshot of studied area in ModelMuse with the wells analysed labelled.

3
Data and Modelling

This chapter aims to present the required components for creating the benchmark model and present the methodology used. The methodology used in this paper encompasses two distinct models: a numerical groundwater flow model and time series analysis using TFN modelling.

3.1 Required Datasets

TFN-modelling is a data-driven modelling tool that relies on quantitative data. (Pezij, et.al., 2020) This subchapter aims to disclose the datasets used to build the time series model.

3.1.1 Head Observations

The head observations from the Haga site were measured as part of the Västlänken project. Wells with longer spans of data are desirable as they help capture natural fluctuations in head levels over time. The wells needed to have active measurements during the simulated timeframe and be integrated in the MODFLOW model. Five wells were selected and are presented in Table 1. The selection of wells includes those placed in both the lower aquifer and wells drilled into bedrock

Table 1 Active wells used in the simulations.

Well	Depth [m]	Placement
HH4001H	*35*	Bedrock aquifer
HH4003H	52	Bedrock aquifer
HH4107U	15	Lower aquifer
HH4297B	32	Lower aquifer
HH4302U	28	Lower aquifer

3.1.2 Stress data

Stress data is utilized in TFN modelling to describe the groundwater situation in the modelling area. This data can include any input that affects the groundwater level, such as recharge, infiltration, or leakage (Collenteur, 2019). In the benchmark modelling, infiltration data originates from MODFLOW simulations. It's worth noting that some of the infiltration data used in the modelling process is theoretical and simulated, reflecting potential scenarios rather than direct observations.

3.1.3 Climate data

Retrieving climate data is crucial for calculating potential evapotranspiration and net precipitation, as it requires both qualitative and quantitative data (Vremec, 2022). It is necessary to have climate data that spans the same period as the well observations to adequately simulate the time series (Collenteur, 2019). Climate data with long time series could be obtained from the Swedish Meteorological and Hydrological Institute, where it was readily available from their website (SMHI, n.d). Table 2 shows the climate data used during the modelling.

Table 2 Downloaded climate data.

Climate data	Measuring station
Global radiation	Gothenburg Sun
Temperature, min and max	Gothenburg A
Precipitation	Gothenburg A
Wind	Gothenburg A
Relative humidity	Gothenburg Landvetter Airport

From SMHI's website, data with a resolution suitable for the aims of this paper was downloaded (SMHI, n.d). The measuring station "Gothenburg A" was the closest to the study area and was initially used. However, global radiation was not measured at this station, so data from the station called "Gothenburg Sun" was utilized instead. The proximity of both these stations suggests that climate data from them are applicable for the Haga area. However, the data series for relative humidity from "Gothenburg A" contained gaps during the period of interest, rendering it unsuitable. Consequently, the measuring station "Gothenburg Landvetter Airport" was selected instead. Despite the distance between the measuring station "Gothenburg Landvetter Airport" and the study area, it was verified that both "Gothenburg A" and "Gothenburg Landvetter Airport" followed a similar trend and could be assumed to be representative. Further details on how the climate data was utilized can be found in chapter 3.2.

3.1.4 Net precipitation

Net precipitation and evapotranspiration are crucial parameters when investigating groundwater recharge (Luetkemeier, Söller, & Frick-Trzebitzky, 2022). Net precipitation is sometimes referred to as recharge; however, it was decided to label it as net precipitation to emphasize its role as potential recharge (SGU, 2019). Actual groundwater recharge can vary depending on factors such as the presence of impervious surfaces in the area (Hernández-Hernández, et.al., 2023). Previous calculations in Gothenburg regarding groundwater recharge have assumed that less than 20% of net precipitation will contribute to groundwater recharge (Sundkvist, 2016). In this project, net precipitation was calculated using Equation 1 to estimate potential groundwater recharge, and adjustments for actual recharge were made during modelling (Rutgersson, Omstedt, & Räisänen, 2002).

$$NP = P - ET$$

Equation 1

NP represents net precipitation (mm/year),
P stands for precipitation (mm/year), and
ET denotes evapotranspiration (mm/year).

3.2 Potential Evapotranspiration

The Python PyEt package was employed to estimate potential evapotranspiration using climate data from the site of interest (Vremec, 2022). PyEt offers 20 different methods for estimating potential evapotranspiration, allowing users to specify the preferred method. The process of collecting the necessary climate data is outlined in chapter 3.1 Required Datasets.

Among the 20 available methods, the Penman method was selected for calculating potential evapotranspiration. The code used for PyEt calculations can be found in Appendix 1. The data

retrieved from SMHI is provided at an hourly interval, necessitating the calculation of daily averages. This step was essential as PyEt computes potential evapotranspiration with daily frequency.

3.3 MODFLOW modelling

A numerical groundwater flow model was designed and compared to a time series model to establish a connection between the two models and assess how well time series analysis allows quantification of leakage into a tunnel. The base model incorporated numerous predefined functions and variables derived from various hydrogeological tests conducted in the study area as part of the tunnel construction project known as Västlänken (Pool, et.al., 2024). Essential features such as stratigraphy and fracture zones were already included in the model. Certain aspects needed to be added or modified to align with the specific objectives of this study.

The modelling of the MODFLOW model was carried out in two steps. First, the previously calibrated base model was further calibrated to incorporate a time-varying recharge boundary. This initial stage of modelling represented the period from 2017.10.01, to 2019.09.21, when tunnel construction had not yet started in Haga. Calibration during this period was performed to match the observed well data. This involved creating a model that accurately represented fluctuations and groundwater levels. In the second stage, the tunnel was added, and the model was run to extract results. With the tunnel included, the model represented the period from 2021.10.01, to 2023.09.31, covering the latest two hydrological years during which the tunnel has been under construction. Adding the tunnel enabled the measurement of changes in groundwater head in response to the tunnel construction.

To have a higher frequency of outputs from the model but still be able to calibrate the model in several steps the time steps for MODFLOW were set to represent one week. The decision to have the time steps to one-week intervals aimed to streamline the modelling process, considering the computational intensity of simulations and the time required for completion with higher time resolution. Comparing the simulated head observations to their observation counterparts required in this case resampling the data. As the model's time steps were equivalent to one week, while the head observation data had a daily sampling interval. Resampling the data at one-week intervals was achieved using the code provided in Appendix 4, which adjusted the sample rate and averaged the results.

Utilizing the MODFLOW package HOB (Head Observation), it was feasible to derive a simulated time series from the MODFLOW model. Pre-existing HOB wells in the base model were investigated and compared to wells that had enough observed data over the periods evaluated. The wells HH4001H, HH4003H, HH4107U, HH4 and HH4 were found to both be active and relevant in the model and have observed data that could be used. The main well was HH4107U since it had the most observed data over both the calibration period and the analysis period.

For the evaluation of correlation between the measured dataset and the simulated dataset generated with MODFLOW, Spearman rank coefficient, r_s, was used to determine the correlation. Spearman rank coefficient is a measurement more representative for datasets with non-linear relationship (Feijóo & Villanueva, 2016).

3.3.1 Calibration in MODFLOW

Initially, the model was configured with a constant head boundary condition, which needed to be replaced with a recharge boundary condition to facilitate the incorporation of time-varying recharge data. The initial model had a constant head boundary which kept a constant GW head in the top layer to simulate a constant addition of GW. The modification to a recharge boundary allowed for the inclusion of recharge variations over time within the model. When incorporating the recharge boundary as an area covering the model, a calibration process was initiated to align the results with those of the base model. It is crucial to distinguish between recharge and net precipitation, where net precipitation can be considered potential recharge (SGU, 2019).

Modelling two years with a starting step as steady state resulted in 105 steps. Table 3visualizes the time steps and the represented date connected to each step. The first steady state step is implemented to stabilize the model according to the input data to represent the time before 2017.10.01. Recharge input for the steady state step were calculated as the average net precipitation for the hydraulic year 2017.10.01-2018.09.31. The time steps consist of a one-week period where the represented date represent the first date of each time step.

Table 3 Time steps with representing date and the recharge input for 2017-2019

Time step	Represented date	Recharge input [m/s]
0	*Steady state*	4.4 E-09
1	2017.10.01	1.0 E-12
2	2017.10.08	1.3 E-08
3	2017.10.15	8.4 E-09
4	2017.10.22	3.8 E-09
…	…	…
105	2019.09.29	1.7 E-08

The recharge input for the model is based on the net precipitation for the period. This net precipitation is calculated as the average weekly net precipitation for the relevant time step. Net precipitation is not the same as recharge; according to previous studies, the infiltration to rock in Sweden can be estimated to be 20% of the net precipitation (Olofsson, et al., 2001). Calibration of the net precipitation amount to be used as recharge input was done iteratively. The final recharge input was set to 25% of the net precipitation. Lower recharge inputs could lead to errors in the model during operation.

The reduction of net precipitation for input into the model was based on two factors: first, the previous estimation of 20% recharge from net precipitation, and second, the iterations in the model, where lowering the recharge input produced more accurate results.

Calculating net precipitation using Equation 1 sometimes resulted in getting a negative value. The negative values can occur during certain months where precipitation is low, and it implies that water is leaving the system. During modelling the negative recharge inputs resulted in errors which lead to the replacement of all negative recharge values with 0. Some of the problems remained after that change and to handle this the recharge input for these weeks were changed again to 1E-12 [m/s]. The recharge input used in the modelling is visualized in Figure 6 and Figure 7. As the model doesn't account for land use it was assumed that recharge was distributed uniformly over the modelled area and the recharge boundary was added to the topmost layer.

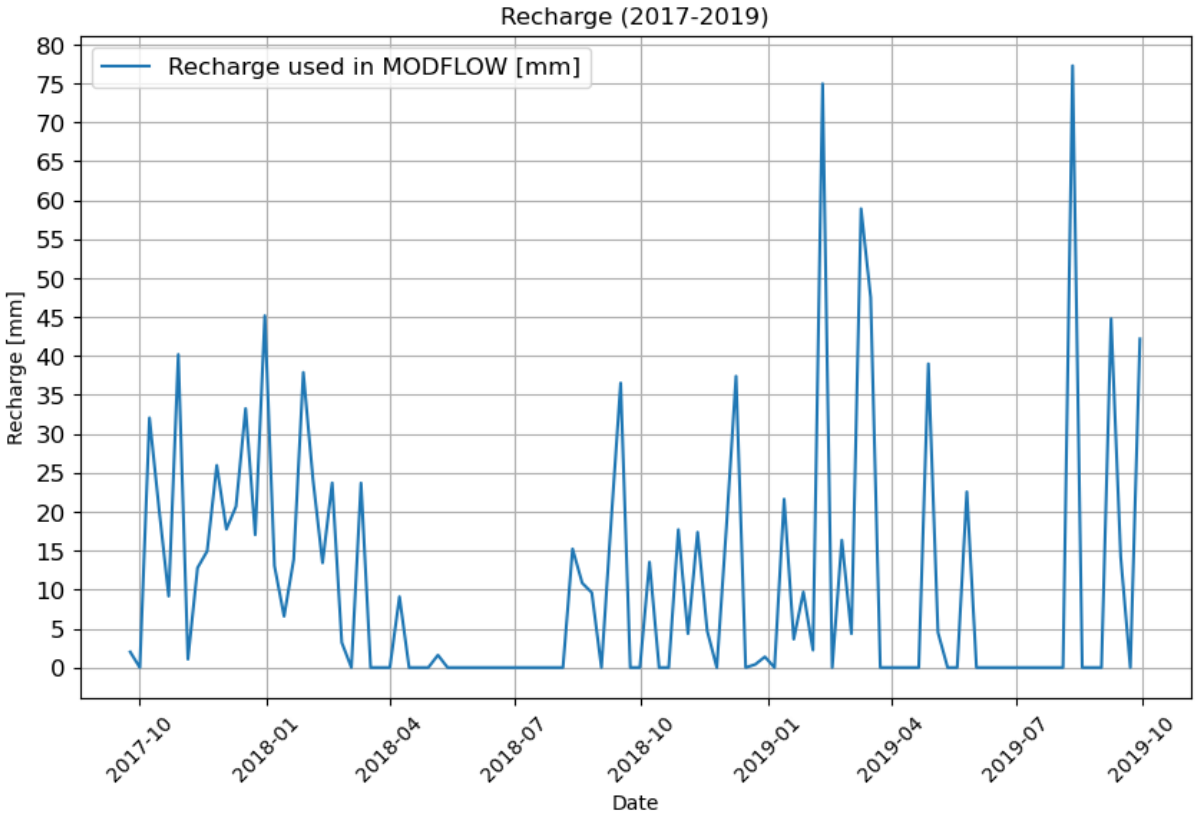

Figure 6: Recharge used in the MODFLOW model for the period 2017-2019.

The first calibration process was done to match the GW head outputs from the model with the recharge boundary compared to the GW head outputs from the base model. When only implementing the recharge boundary a water accumulation was observed within the first layer and above the surface. To manage this problem a drain layer was inserted as a polygon above the model surface. This drain layer will represent the stormwater and drainage network that would naturally happen. The application of the drain layer was tested in different ways to reach the best effect on the model. Polyline representing existing drains and combinations of smaller polygons were tested. A larger polygon covering the entire area were resulting in the best modelling results and therefore applied.

Calibrations were initially carried out in steady state with hydraulic conductivity for both the topmost layer and the drain polygon as changeable parameters. The goal in this stage were to get a rough estimation of the parameters and were done by comparing GW head in layer 1, 3 and 6 with the base model.

After getting a rough estimate of the hydraulic conductivity for the first layer and the drain polygon the time steps were added. In the transient calibration step the model was further calibrated to match the observed well data by adjusting the hydraulic conductivity. Additionally, storativity was adjusted with modifications of specific storage and specific yield in the model. By adjusting the storativity, it becomes possible to modify the characteristics of the response, either by delaying or increasing it. Specific storage quantifies how much groundwater a particular soil layer can release concerning a decline in hydraulic head (Kuang, et.al., 2020). Were specific yield measures how much water is released through gravitational drainage (Cheng, et.al., 2020). While adjusting the values of these parameters to replicate the observed GW fluctuations it was crucial to keep the parameters within reasonable limits.

Through different model iterations, certain parts of the groundwater variations could be somewhat replicated.

The parameter calibration process was done by changing one or more parameters before running the model. The results were analysed both visible and by calculating Spearman's correlation coefficient, r_s, before making further adjustments and running the model.

3.3.2 Addition of a tunnel

The addition of a tunnel in the model was done with two objectives: to analyse the incorporation of a tunnel in MODFLOW and to use the generated time series as inputs in Pastas. The analysis of MODFLOW results covered the hydraulic years from 2021 to 2023. When creating the time series for Pastas with MODFLOW, an additional year was included, covering the hydraulic years from 2020 to 2023. This extension allowed the timeframe to be split into two 18-month phases. During the first 18 months, the model was simulated without the tunnel being activated, and during the latter 18 months, the tunnel was activated.

After calibration, the model period was adjusted to the hydraulic years according to the simulation objectives. Table 3 includes the time steps, each representative date, and the recharge inputs for the model according to the simulation over 2021-2023. For the simulation between 2020-2023, the additional hydraulic year was treated the same way as the 2021-2023 period. Time step 0 has the average net precipitation for the hydraulic year 2021-2022. Apart from the changed recharge inputs, the model retains the variables from the calibrated model for the period between 2017-2019. The recharge input used in the modelling, which is 25% of the calculated net precipitation according to the calibrated model of 2017-2019, is visualized in Figure 10.

By adding the tunnel to the model, it was possible to estimate the effects of the real-life counterpart. The tunnel added is a fictive representation of the actual tunnel, which is still under construction.

Table 4 Time steps with representing date and the recharge input for 2021-2023

Time step	**Represented date**	**Recharge input [m/s]**
0	*Steady state*	5.8 E-09
1	2021.09.26	5.3 E-09
2	2021.10.03	4.8 E-08
3	2021.10.10	8.2 E-09
4	2021.10.17	1.0 E-12
…	…	…
105	2023.09.24	2.1 E-08

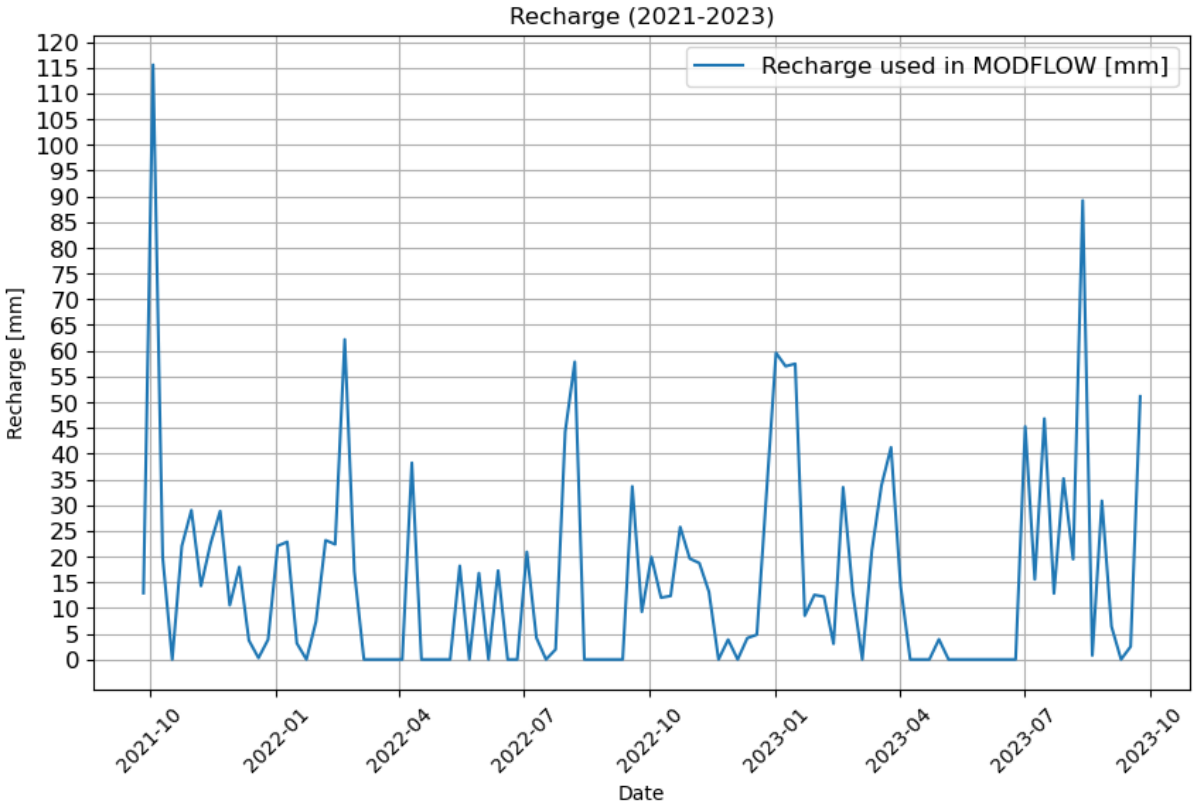

Figure 7: Recharge used in the MODFLOW model for the period 2021-2023

Applying a tunnel to the model were done using a polyline as a drain. The polyline was created along the area where the tunnel is being built as can be seen in Figure 8, along with the wells and their proximity to the tunnel. Based on available construction plans for the model area (Trafikverket, 2020), the tunnel bottom was placed 20 m below sea level. Hydraulic conductivity for the tunnel is based on a triangular distribution were 3E-9 were the most likely and therefore applied as the conductance for the drain acting as the tunnel in the model.

Figure 8 Snapshot of the modelled area with the proposed tunnel location denoted by the yellow line.

3.4 Time series modelling

The time series modelling approach employed in this thesis is based on Transfer Function Noise (TFN) modelling. TFN modelling, short for Transfer Function Noise modelling, is a method suitable for capturing the dynamic behaviour within a system with multiple input variables, where the output demonstrates a nonlinear response to these inputs (von Asmuth, Bierkens, & Maas, 2002).

For implementing TFN modelling, the Python package Pastas was utilized within this study. Pastas is an open-source project offering the essential framework for analysing hydrological and hydrogeological time series data (Collenteur, 2019).

3.4.1 Transfer function noise modelling

Transfer Function Noise (TFN) modelling is a technique utilized to assess transients by transforming one or more time series with uniform time intervals into a single time series through a statistical model (Collenteur, 2019).

According to (Collenteur, 2019), a TFN model in its most fundamental form can be represented by Equation 2.

$$h(t) = \sum_{m=1}^{M} h_m(t) + d + r(t)$$

Equation 2

h(t) represents the measured head level,
m denotes the contribution of a specific stress to the head level,
d signifies the base elevation of the model,
r(t) represents the residuals.

From Equation 2, it is evident that multiple stresses can be applied to the model, each with its individual weighting contributing to the observed head level. Equation 3 allows for the delineation of the individual impact of each stress applied.

$$h_m(t) = \int_{-\infty}^{t} s_m(\tau)\theta_m(t-\tau)d\tau$$

Equation 3

$h_m(t)$ is the contribution from the stress m,
θ_m denotes the response function for the stress m,
s_m denotes the time series for the stress m added.

Equation 3 delineates the convolution operation, which combines the time series associated with a specific stress and the response function corresponding to the applied stress. In essence, this operation yields a new function valid only over the overlapping time spans of the two input functions (MathWorks, n.d). In this case equation 3 represents the maximum activation of the response function during the given stress period.

In TFN modelling, noise refers to stochastic variations that may disrupt the relationship between the model's input and output (von Asmuth, Bierkens, & Maas, 2002). While noise can potentially hinder model accuracy by introducing disturbances, incorporating noise into the

model enhances its resilience, enabling the generation of reliable output even with data of lesser quality.

Residuals represent the disparity between the modelled data and the observed data (von Asmuth, Bierkens, & Maas, 2002). They play a pivotal role in assessing the model's goodness of fit, with ideally stochastic distributions indicating the absence of discernible patterns in the residuals. Any discernible pattern in the residuals suggests potential flaws in the model that require further refinement (Law & Jackson, 2017). Moreover, residuals should center around zero; greater deviations from zero imply significant discrepancies between the modelled and observed values, indicating inaccuracies in the model.

3.4.2 Time Series Modelling

Data from each well was visually analysed (Barthel, Haaf, Nygren, & Giese, 2022) allowing for the identification and treatment of irregularities such as uneven measuring intervals, outliers, or data gaps. Subsequently, running the model provides an opportunity to assess its accuracy through the generated output file. The initial model with no additional stresses typically exhibits lower model accuracy which is expected to improve with the addition of additional stresses such as leakage (Collenteur, 2019). The TFN model were evaluated using the coefficient of determination, R^2. This were done as the standard setting by Pastas 1.5.0.

3.4.3 Calibration process

The Pastas model used data from 2020-2023 and there was a calibration and validation period for the model. The purpose for adding the calibration period is train the model on historical data with the aim of adjusting parameters with the end goal of improving the model accuracy. The validation period is then added, where new data which wasn’t used in the calibration period to confirm the calibration. By adding validation data, it is more likely that the model doesn’t predicts and overfit. For the Pastas model used there was a calibration period of set to 18 months and validation period of 18 months.

4
Results

This chapter aims to present the results of the modelling process for all models incorporated within the scope of this thesis paper. The chapter will detail the outcomes from the raw time series comparisons, MODFLOW results, and the Pastas modelling results.

4.1 MODFLOW 2017-2019

Figure 9 shows the result from the calibration for well HH4107U after iterations aiming to roughly calibrate the simulation according to the observed data. As can be seen the simulated head have more distinctive peaks and troughs compared with the observed data. In order to manage this, further calibration was done with the focus on storativity. Notable is that the observed data is modified by increasing the GW head with 1 meter. This is done to be able to analyse and calibrate the trends of the GW head over time.

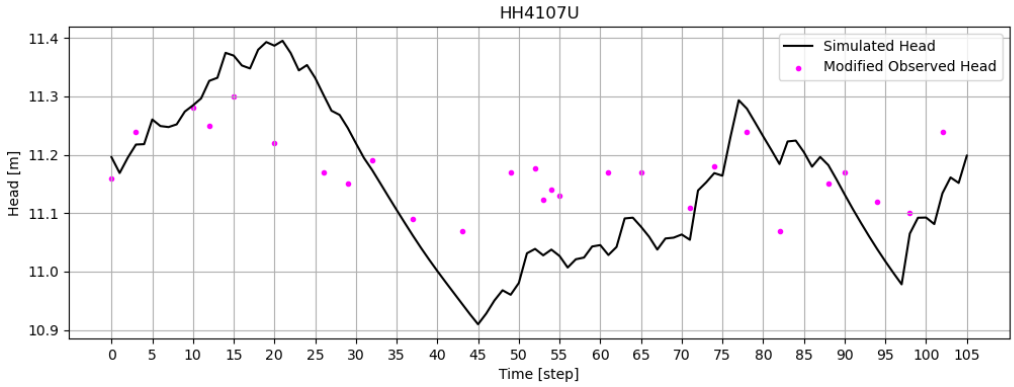

Figure 9 Simulated time series after first stage of calibrations.

The iterative process of calibrating the model included changing the parameters for different inputs one by one or several at a time and evaluating the result. The parameters that were calibrated are listed in Table 5 were Kx represent hydraulic conductivity, Sy represent specific yield and Ss represent specific storage. The tested interval of the parameters is based on literature values for the specific material. Layer 2 is for instance clay that according to (Woessner & Poeter, 2020) can be expected to have a specific storage in the range of 0.01 to 0.18.

Table 5 Parameters and the values used in the calibration process.

Object	Parameter	Original value	Tested interval	Final value	Unit
DRAIN	*Kx*	*Added parameter*	1 E-8 – 1 E-5	1 E-7	[m/s]
Layer 1	*Kx*	1 E-8	1 E-8 – 1 E-4	1 E-5	[m/s]
Layer 1	*Sy*	0.2	0.13 – 0.5	0.5	[-]
Layer 2	*Sy*	0.02	0.01 – 0.18	0.14	[-]
Layer 3	*Sy*	0.2	0.13 – 0.47	0.45	[-]
Layer 4	*Sy*	0.0001	0.0001 – 0.05	0.0004	[-]
Layer 1	*Ss*	1 E-6	1 E-6 – 3 E-6	1 E-6	[1/L]
Layer 2	*Ss*	1 E-6	1 E-6 – 3 E-6	1 E-6	[1/L]
Layer 3	*Ss*	1 E-5	1 E-5 – 3 E-5	1 E-5	[1/L]
Layer 4	*Ss*	1 E-5	1 E-5 – 3 E-5	1 E-5	[1/L]

When calibrating the MODFLOW model, the observed data and the simulated data from the model were compared. For the period from October 1, 2017, to September 30, 2019, no observations were gathered for the wells HH4297B and HH4302U. The best correlation between the observed and simulated data was found for well HH4103H, with a r_s of 0.73.

Comparing the simulated and observed data showed that there exists a discrepancy between the time series, as the simulated head levels were offset by approximately 1 meter from the observed data points. When the simulated data series was adjusted by roughly 1 m the results improved and yielded a more favourable r_s as can be seen in Figure 10.

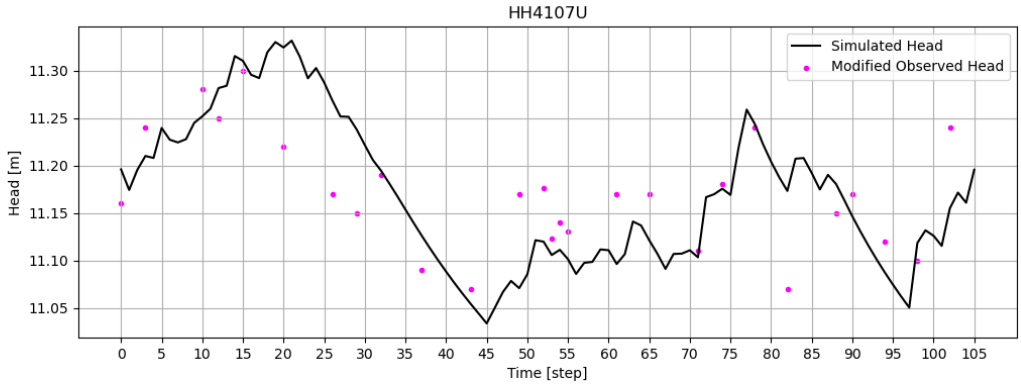

Figure 10 Modified observed head and simulated head for HH4107U, 2017.10.01 - 2019.09.30.

The simulated data from well HH4001H did not follow the same trend as the observed data and was not analysed for correlation. In Appendix 6 - Appendix 8 simulated heads are compared to observations for all wells. All wells analysed for the period from October 1, 2017, to September 30, 2019, are listed in Table 6.

Table 6 Correlation analyses for all wells 2017.10.01 - 2019.09.30

WELL	**Comment**	**r_s**
HH4297B	*No observed data for the period.*	-
HH4107U	*Observed head increased with 1.0 m.*	0.68
HH4302U	*No observed data for the period.*	-
HH4001H	*Simulated data don't follow the trend of observed data.*	-
HH4003H	*Observed head decreased with 1.0 m.*	*0.73*

Observed data for HH4297B and HH4302U are not available for the period before tunnel construction, however an analysis of the simulated head can be conducted in comparison to HH4107U. All three of these wells are near each other and are of similar character. Based on this, it is reasonable to assume that the wells show similarity and according to Figure 11, this is the case. While the simulated values showed similar characteristics it cannot be validated

through observed data since two of the wells lack observation data for this period.

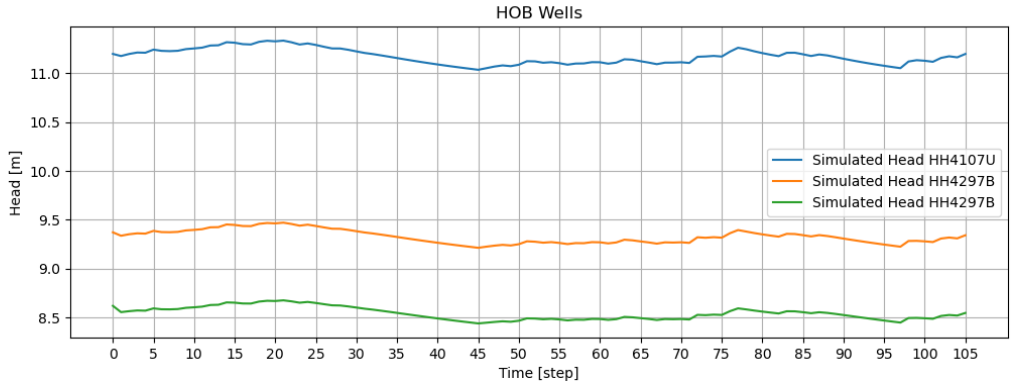

Figure 11 Simulated head for HH4107U, HH4297B and HH4297B

4.2 MODFLOW 2021-2023

For the period from October 1, 2021, to September 30, 2023, observed GW head data are available for wells HH4297B, HH4107U, and HH4302U, which can be analysed. For all three wells, some modifications were needed to the observed head data to align simulated and observed values at the same level. The correlation has decreased compared to before the tunnel construction. The best correlation between simulated and observed head was observed for well HH4297B, with a r_s of 0.58. The difference between observed head and modified observed head, and its impact on the correlation analysis, can be seen in Figure 12 and Figure 13. All wells observed head and modified observed head can be found in Appendix 9 to Appendix 14.

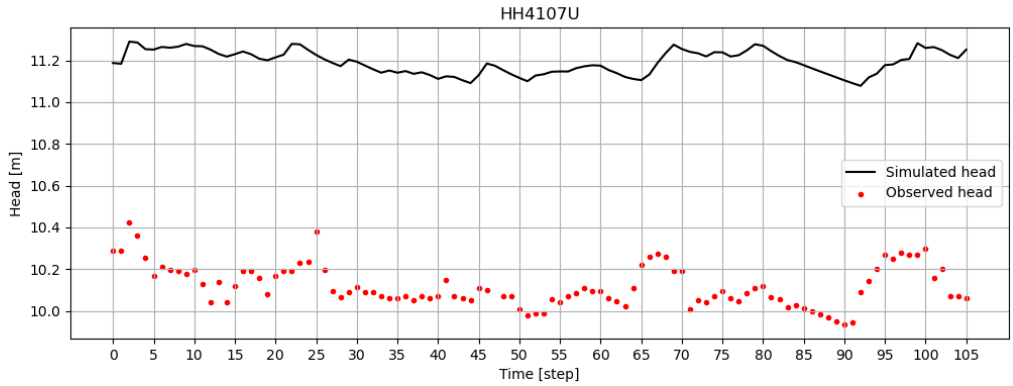

Figure 12 Observed head and simulated head for HH4107U, 2021.10.01 - 2023.09.30.

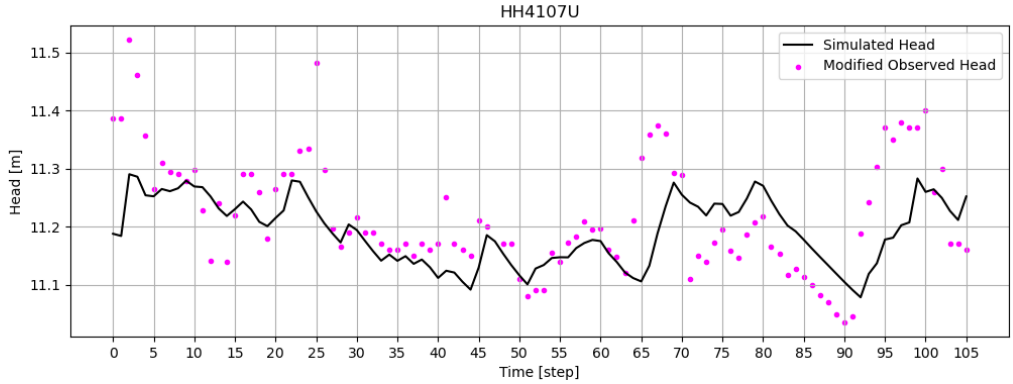

Figure 13 Modified observed head and simulated head for HH4107U, 2021.10.01 - 2023.09.30.

Plots of observed head, modified observed head, and simulated head for wells HH4297B and HH4302U can be found in Appendix 10 and Appendix 11. All wells analysed for the period from October 1, 2021, to September 30, 2023, are listed in Table 7.

Table 7 Correlation analysis for all wells 2021.10.01 - 2023.09.30

WELL	Comment	r_s
HH4297B	*Outliers removed in the observed data.*	0.58
HH4107U	*Observed head increased with 1.1 m.*	0.50
HH4302U	*Observed head increased with 1.0 m.*	0.50
HH4001H	*No observed data for the period.*	-
HH4003H	*No observed data for the period.*	-

4.2.1 Influence of tunnel on GW level

After adding the tunnel to the model, a change in GW head was observed for all wells. The difference between the two scenarios, with and without a tunnel, appeared parallel. Figure 14 illustrates that the two scenarios act as parallel lines over the simulated period. All wells simulations with and without a tunnel can be found in Appendix 15 to Appendix 19.

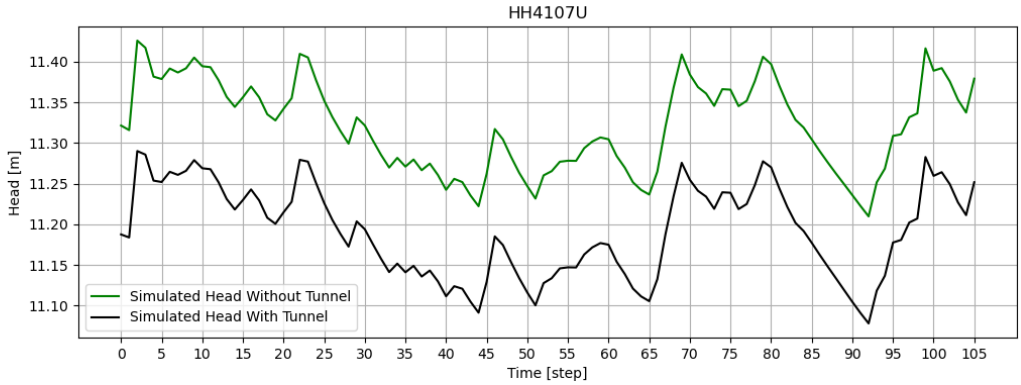

Figure 14 Simulated head without a tunnel and simulated head with a tunnel for HH4107U.

The average change in GW over the simulated period for all wells is presented in Table 8. The variation between the largest and smallest change is calculated and presented as "Variation." From the plots of the changed GW head, as shown in Figure 14, they appear to be parallel. The calculated variation ranges between 9 mm and 38 mm, indicating that the two scenarios closely follow each other.

The average GW changes for the well's ranges between 0.13 meters and 1.16 meters. This can be compared to the guidelines for the project stating that the GW level change due to the project can´t have a large negative impact on the surrounding area (Trafikverket, 2013). A lowering of GW of 0.13 m can have a negative effect and a change of around one meter will have a negative impact in an urban environment.

Table 8 Average GW head change and variation for all wells

WELL	Average GW head change [m]	Variation [mm]
HH4297B	- 0.20	38.0
HH4107U	- 0.13	10.4
HH4302U	- 0.18	19.6
HH4001H	*- 0.53*	*8.95*
HH4003H	*- 1.16*	*58.9*

4.2.2 Variation due to conductivity of tunnel

It was noted that the hydraulic conductivity of the tunnel could vary, but the most probable conductivity was estimated to be 3E-9 m/s. Figure 15 depicts well HH4107U most likely conductivity plotted in black, with the lowest conductivity estimated by Trafikverket (2020) in blue and the highest in red. All wells' plots of different conductivity can be found in Appendix 20 to Appendix 24. The variation in hydraulic conductivity will result in different changes in GW head.

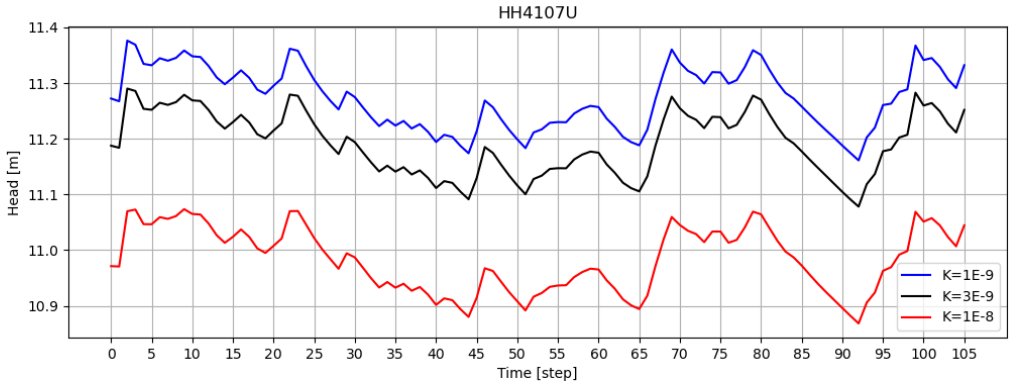

Figure 15 Different hydraulic conductivity for the tunnel, HH4107U.

Table 9 presents the interval between changes in head due to the highest or lowest hydraulic conductivity. "Δ to lowest" describes the change in GW head from the most likely conductivity to the lowest, with a positive value representing an increased GW head. Similarly, "Δ to highest" shows the change from the most likely to the highest estimated conductivity for all wells. The last row describes the total interval of GW head between the lowest and highest conductivity. Observation Well HH4003H, being the closest to the tunnel, will also experience the most significant impact of a changing hydraulic conductivity. Conversely, for wells further away from the tunnel, the changed hydraulic conductivity will have a smaller effect on the GW head.

Table 9 Difference in head due to hydraulic conductivity.

WELL	Δ to lowest [m]	Δ to highest [m]	Total Δ [m]
HH4297B	0.13	- 0.33	0.46
HH4107U	0.08	- 0.21	0.29
HH4302U	0.12	- 0.30	0.42
HH4001H	0.33	- 0.88	1.21
HH4003H	0.73	- 1.76	2.49

The GW head in relation to hydraulic conductivity of the tunnel is plotted in Figure 16 for all analysed wells. The plots show a linear trend with a declining in GW head with higher hydraulic conductivity. Correlation between the linear trends and the simulated values range from 0.90 to 0.96. Distance to the tunnel can be seen to have an impact since the wells closer to the tunnel have a larger decrease in head compared to the wells further away.

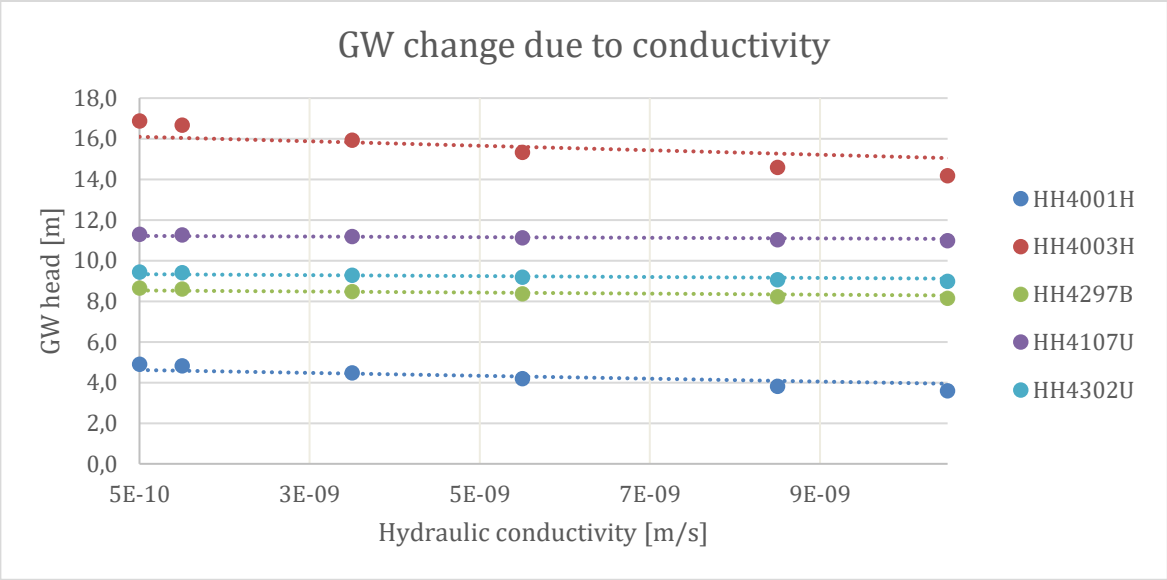

Figure 16 GW change due to change of tunnels hydraulic conductivity.

4.2.3 Leakage data

The MODFLOW model calculated synthetic leakage as the difference in water rerouted with and without the tunnel. Figure 17 shows the total leakage data over the last 18-month of the period between 2020-10 and 2023-09, with the start in 2022-04. This synthetic leakage was then used as a stress input for the Pastas model.

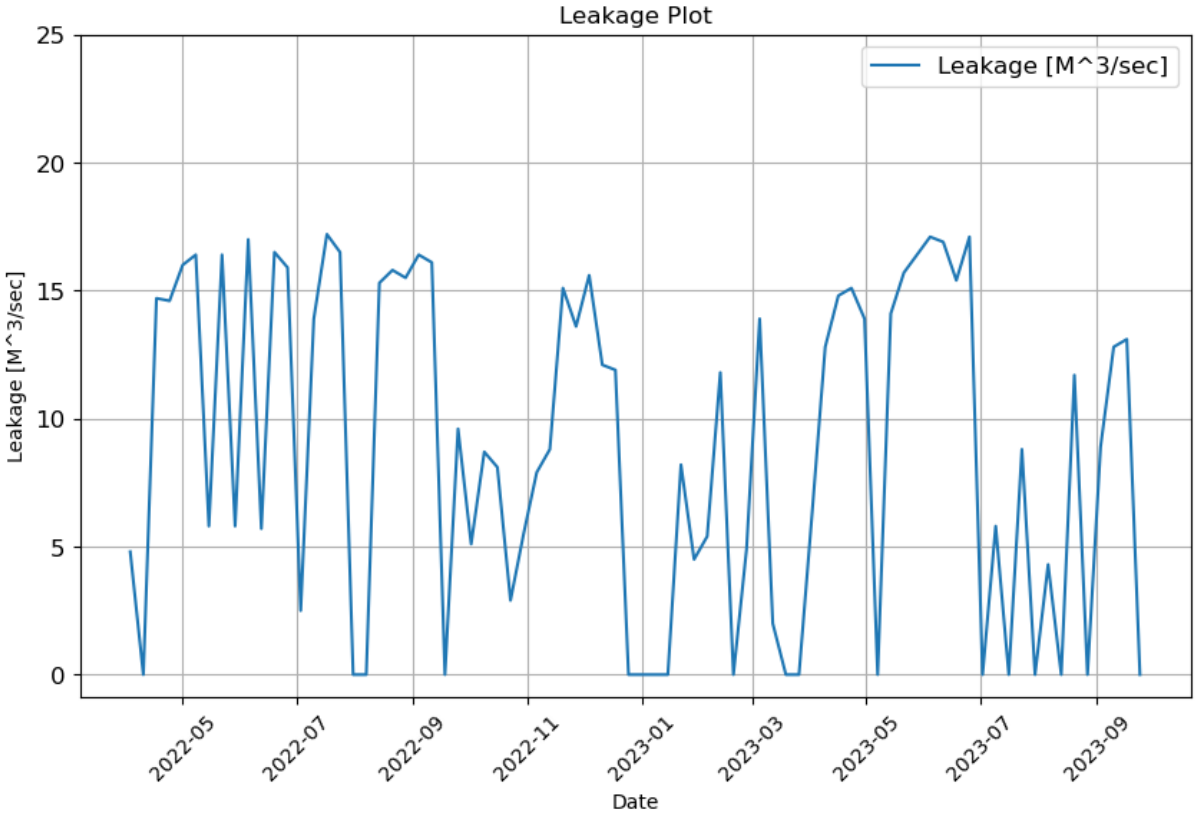

Figure 17: Synthetic leakage derived from the MODFLOW model.

4.3 Pastas model results

This chapter aims to present the results from the Pastas modelling for the available wells. Simulations was performed for the period 2020-2023 as this period encompasses a period where the construction hadn’t started, but it also includes a period where the tunnel construction has started. By using the period 2020-2023 it is possible to see the GW drawdown induced by the tunnel construction. For the Pastas model a calibration period of 1 year was implemented, and 2 years were used as validation data.

The Pastas model was simulated in 2 scenarios. Where the model was initially run without leakage data. The model was then tun with leakage data, and the reason for this is connected to Chapter 3.4.1 as adding mode stresses to the model should yield a better model fit. The code used to run the Pastas model without leakage data is presented in Appendix 2, and the code for the Pastas model with leakage data is presented in Appendix 3. Regarding leakage data it was calculated as the difference in water rerouted by the drains from the MODFLOW model for the scenario where the tunnel was implemented and the scenario where the tunnel wasn’t present.

4.4.1 Simulated well HH4297B

Observation well HH4297B was simulated for the period 2021-2023. For this period the model shows there exist a high correlation between the modelled data and the time series from the MODFLOW model, see figure 18. It is visualized in figure 18 that there is a drawdown in GW because of the tunnel construction, where the GW head is lowered by approximately 0.3 m.

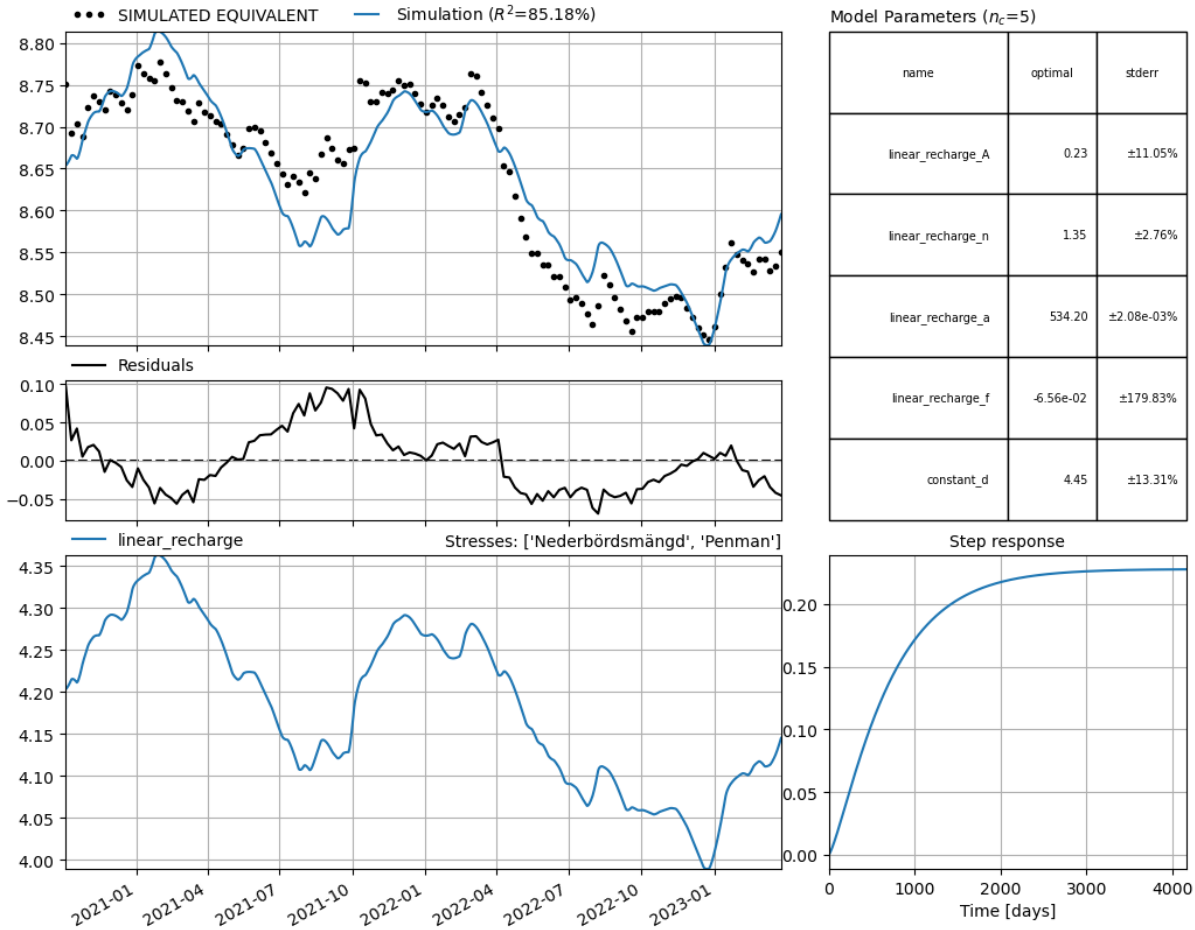

Figure 18: Model output for the simulated base model for well HH4297BH, after tunnel construction.

Observing Figure 18 it is possible to deduce that there is likely a stress which needs to be added to account for the missing model fit.

4.4.2 Simulated well HH4297B with leakage stress

Running the model with leakage added the Pastas model shows a better model fit (see figure 19) compared to the Pastas model without leakage data (see figure 18). This iteration of the pastas model is also capable of displaying the GW drawdown induced by tunnel construction.

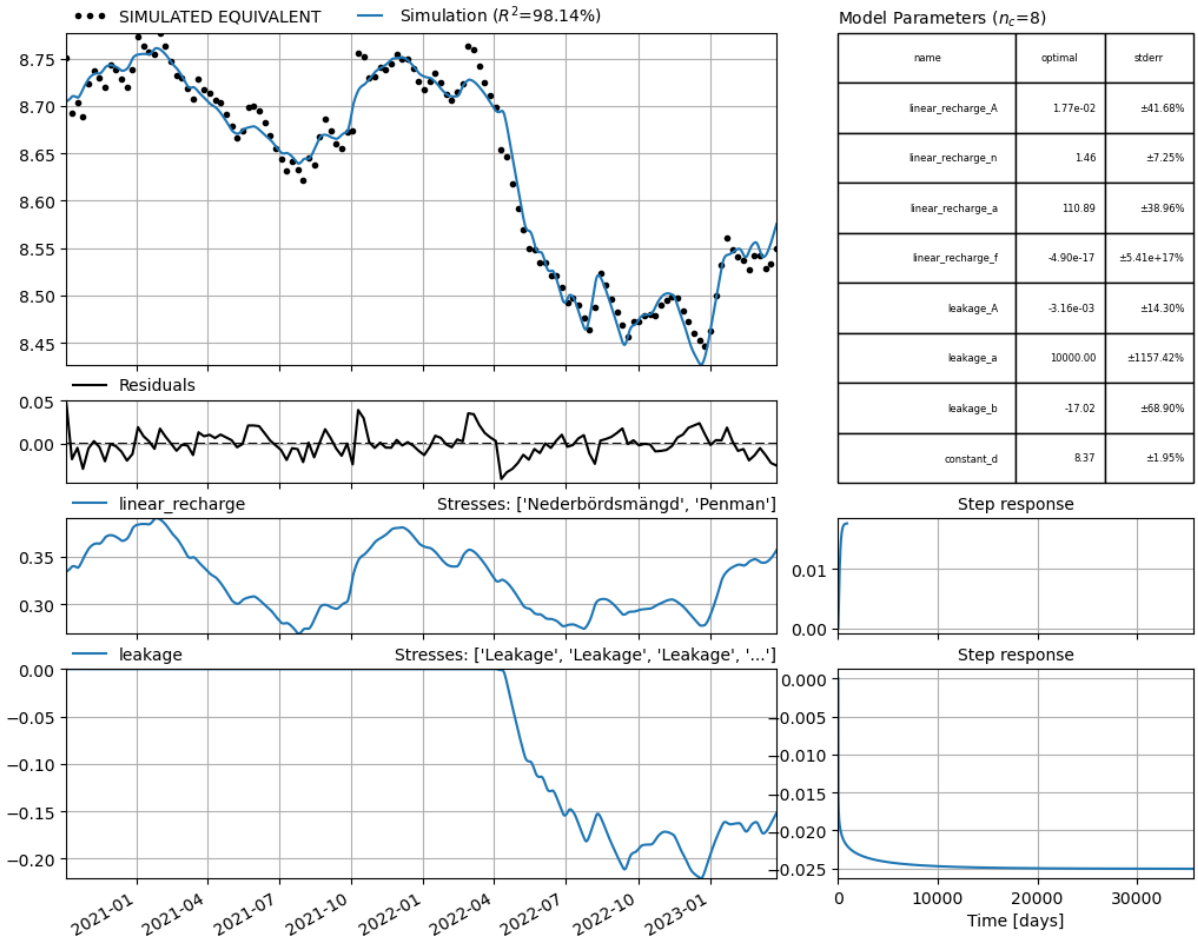

Figure 19: Model output for the calibrated simulated model for well HH4297BH, after tunnel construction.

4.4.3 Simulated well HH4107U

Observation well HH4107U was simulated for the period 2021-2023. For this period the model shows that there exists a high correlation between the modelled data and the time series from the MODFLOW model, see figure 20. It is visualized in figure 20 that there is a drawdown in GW because of the tunnel construction, where the GW head is lowered by approximately 0.4 m.

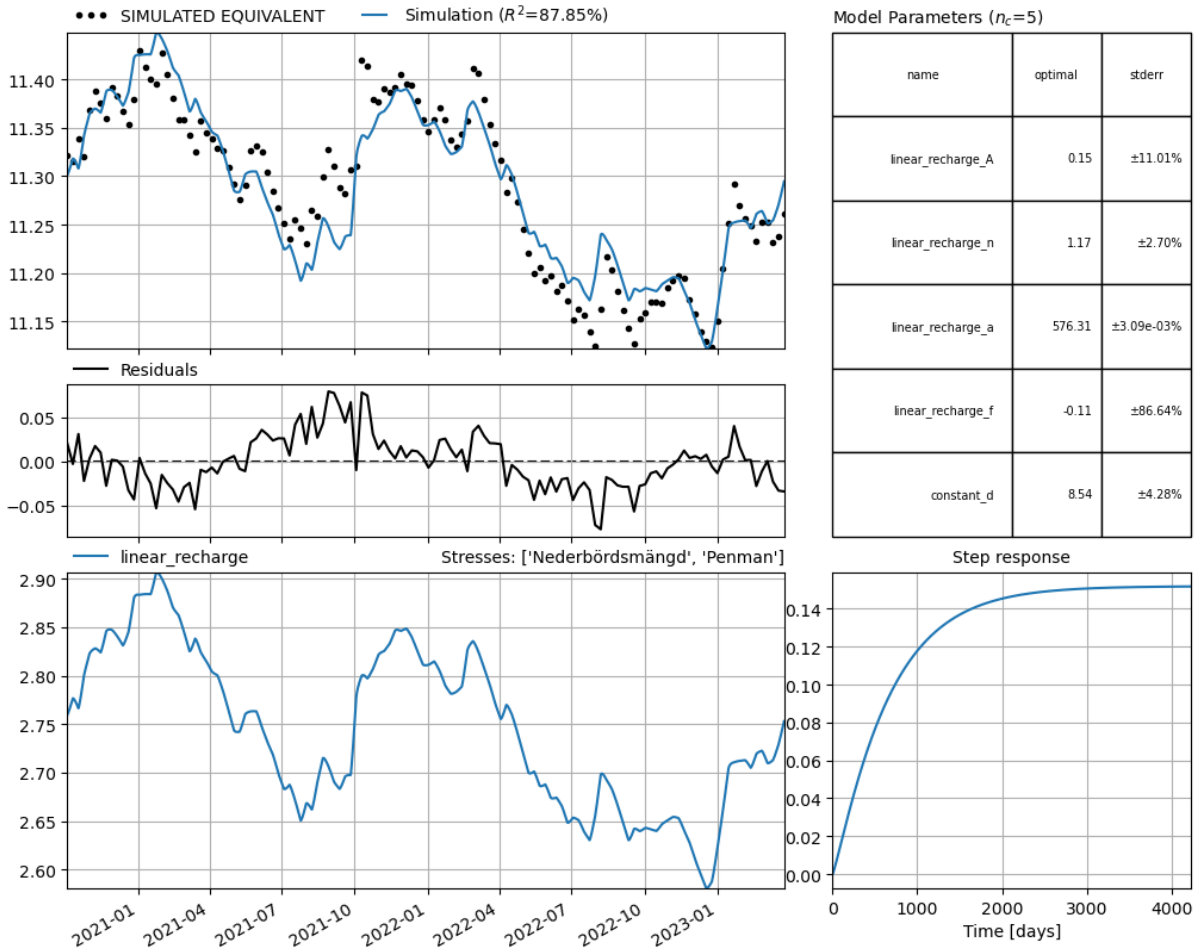

Figure 20: Model output for the simulated base model for well HH4107U, after tunnel construction.

4.4.4 Simulated well HH4107U with leakage stress

Running the model with leakage added the Pastas model shows a better model fit (see figure 21) compared to the Pastas model without leakage data (see figure 20). This iteration of the pastas model is also capable of displaying the GW drawdown induced by tunnel construction.

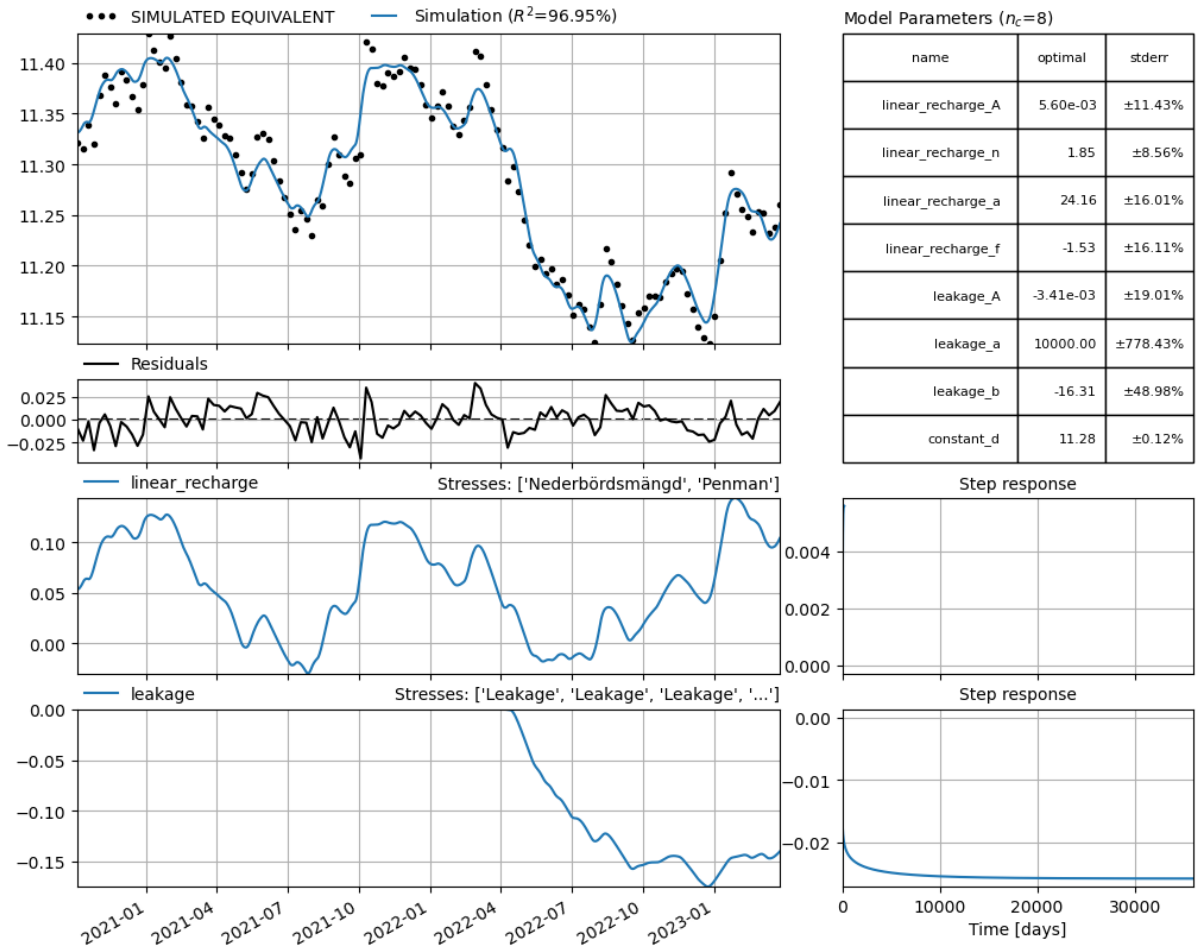

Figure 21: Model output for the calibrated simulated model for well HH4107U, after tunnel construction.

Observing Figure 21 it is possible to deduce that there is likely a stress which needs to be added to account for the missing model fit.

4.4.5 Simulated well HH4302U

Observation well HH4302U was simulated for the period 2021-2023. For this period the model shows that there exists a high correlation between the modelled data and the time series from the MODFLOW model, see figure 22. It is visualized in figure 22 that there is a drawdown in GW because of the tunnel construction, where the GW head is lowered by approximately 0.35 m.

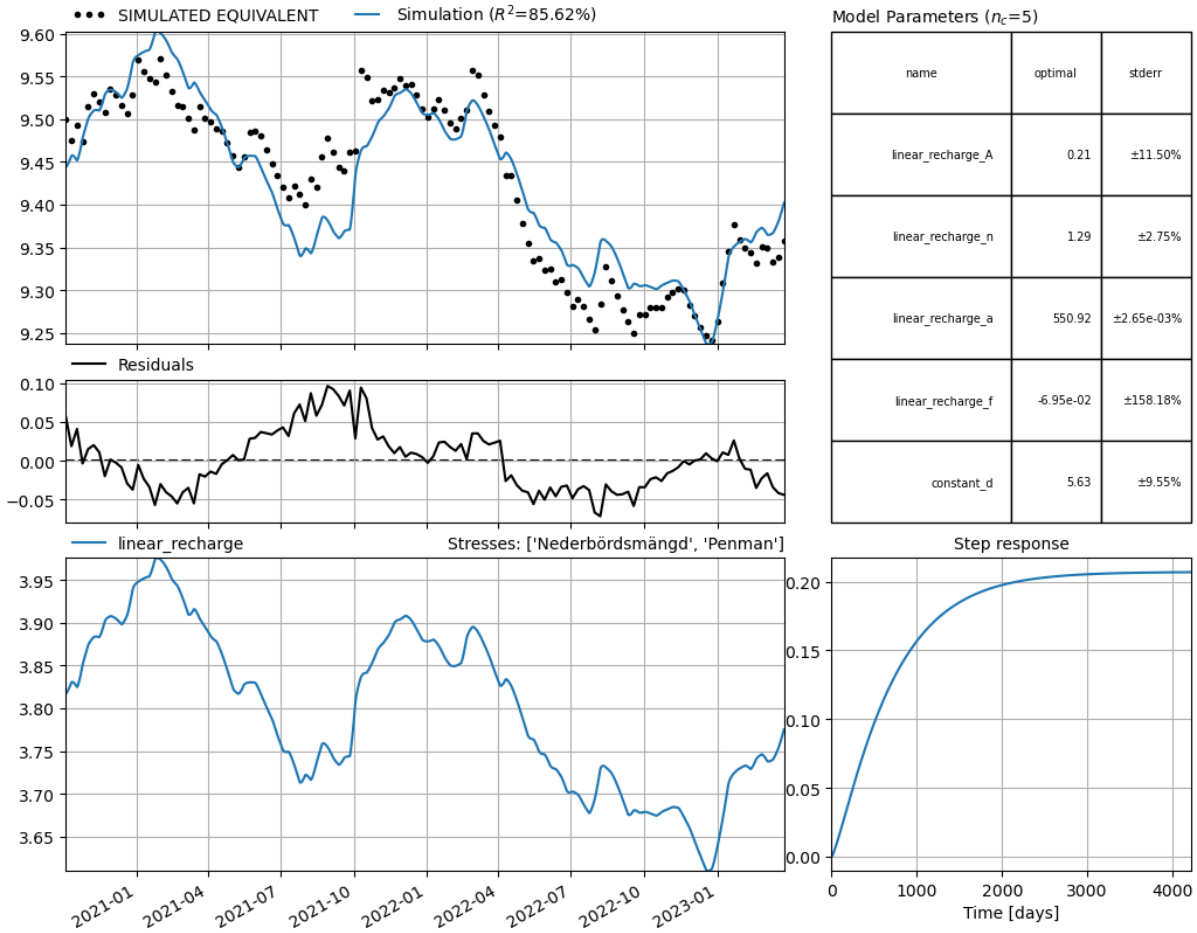

Figure 22: Model output for the simulated base model for well HH4307U, after tunnel construction.

4.4.6 Simulated well HH4302U with leakage stress

Running the model with leakage added the Pastas model shows a better model fit (see figure 23) compared to the Pastas model without leakage data (see figure 22). This iteration of the pastas model is also capable of displaying the GW drawdown induced by tunnel construction.

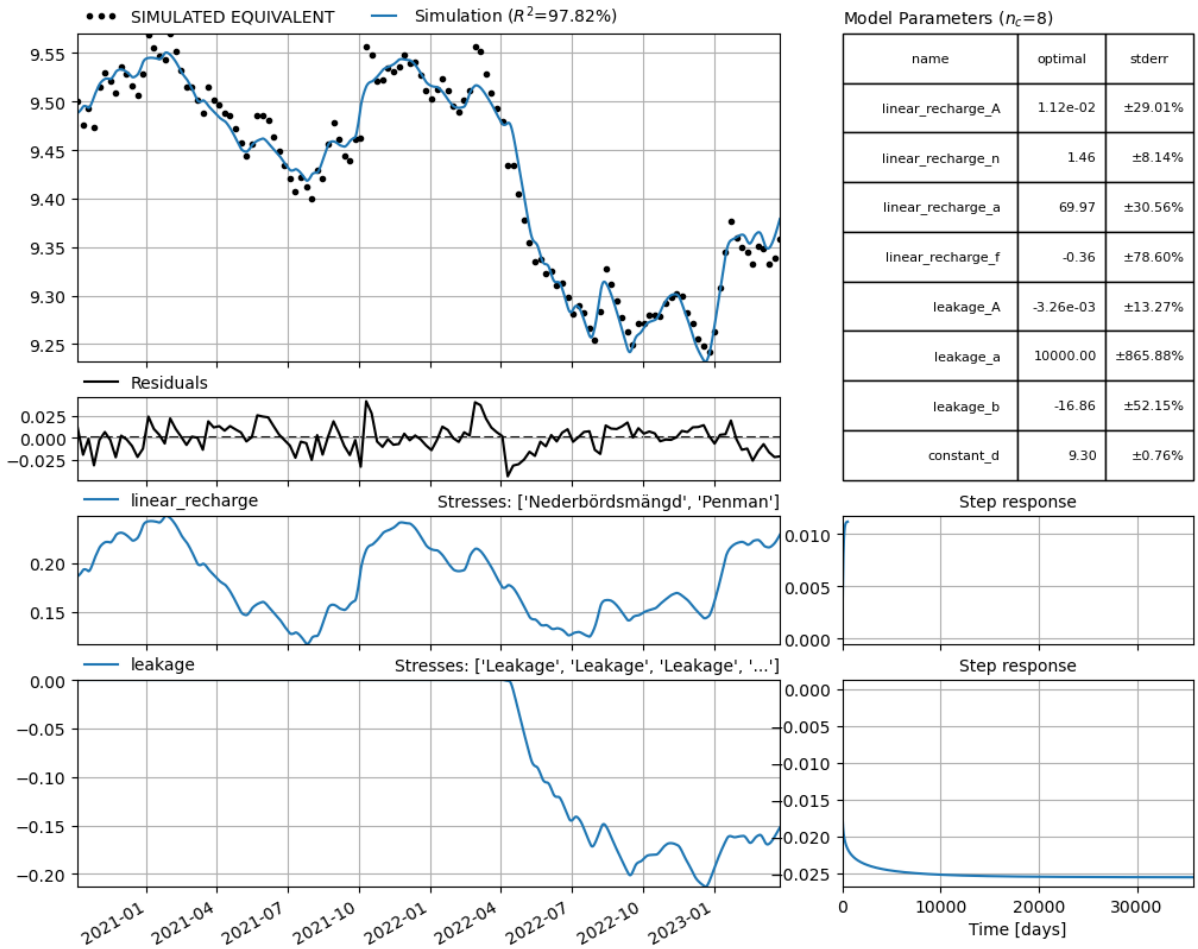

Figure 23: Model output for the calibrated simulated model for well HH4197U, after tunnel construction.

Observing Figure 23 it is possible to deduce that there is likely a stress which needs to be added to account for the missing model fit.

4.4.7 Measured well HH4297B

For observation well HH4297B had observed data for the specified period, which allowed for simulation using measured data rather than synthetic data. The simulation using the measured data shows a high correlation between the simulations from Pastas and the measured GW head levels (see figure 24). A major difference between the synthetic head levels and the measured head levels is that there exists no leakage data available for the measured time series. Since there exists no leakage data for the measured time series the model accuracy for the measured time series cannot be improved upon. Even if leakage data was available, it would not guarantee that the measured well would exhibit the same behaviour as the modelled well using synthetic data.

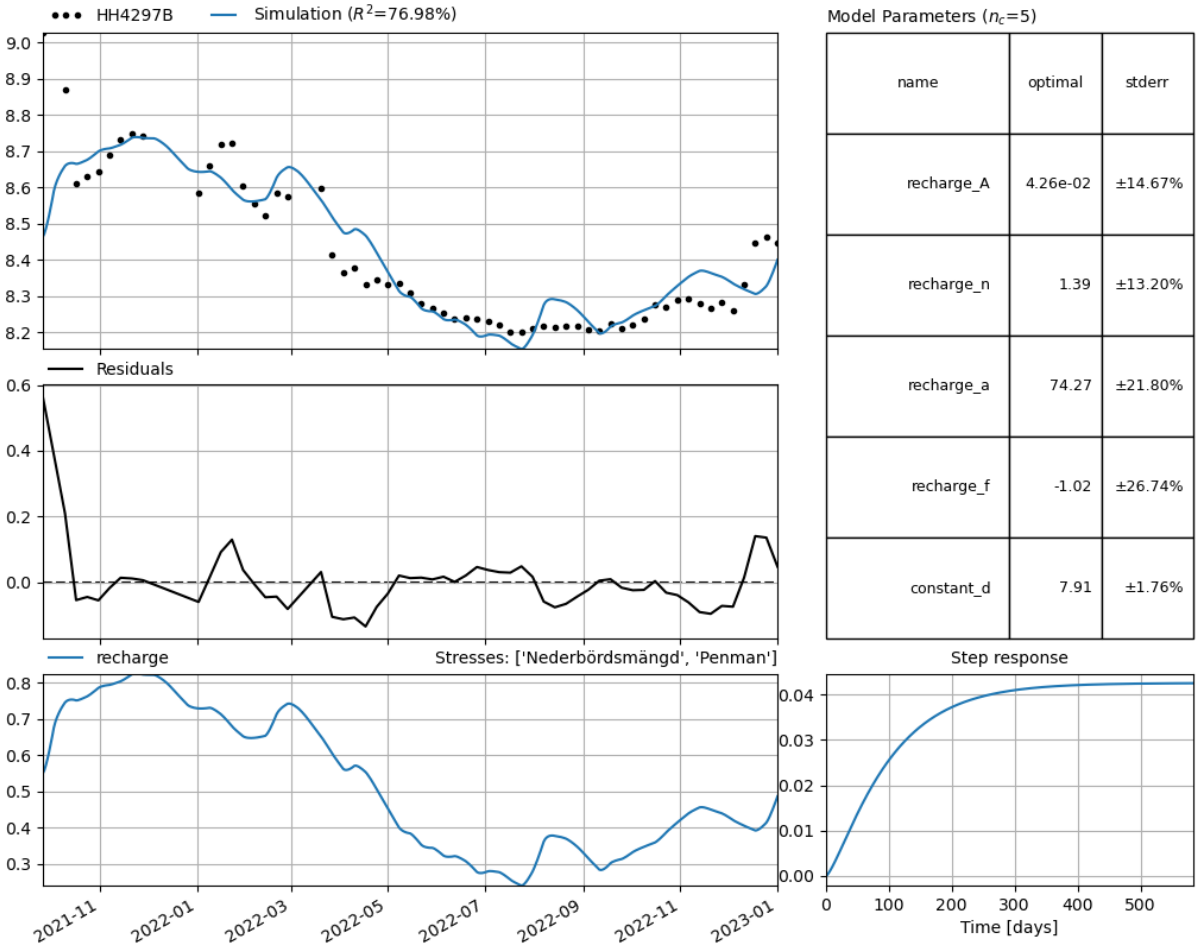

Figure 24: Model output for the measured base model for well HH4297B, after tunnel construction.

4.3.8 Summary of pastas model

The Pastas model shows good model fit for all the scenarios simulated. Where it is was shown that adding more stresses in this case leakage data improved the results. It was possible to see that the tunnel construction had an impact on the GW head levels. Were the drawdown from the tunnel ranged from 0.3 m to 0.4 m.

As the Pastas model uses a calibration period of 1 year and then a simulation period of 2 years it was reasonable to calculate how well the model fit was for the specific part of the Pastas model. In table 10 the Spearman ranking coefficient r_s for the different wells during the different stages is presented. In table 10 it is possible to see that the model fit is good for the different stages of the model for all the wells simulated.

Table 10 Spearman ranking coefficient for calibration and simulation periods.

WELL	**r_s Calibration**	**r_s Simulation**
HH4297B	0.90	0.97
HH4107U	0.94	0.85
HH4302U	0.93	0.94

5
Discussion

This chapter will provide the main findings of the modelling process and which processes and uncertainties have influenced the results from the modelling process.

5.1 Constructing a real-life benchmark model

Calibration of the MODFLOW model for the period 2017-2019 resulted in good agreement between observed and simulated GW head data for various wells. The simulated GW head were able to show similar temporal dynamics as the observed data. The general pattern of groundwater fluctuations due to recharge of the observed head were picked up by the simulated data. The need to lower the observed head data to achieve a reasonable correlation between the observed and synthetic time series suggests that the MODFLOW model may not fully capture certain aspects of the study area.

Since the Haga site is an urban area the soil and bedrock are not undisturbed and previous building sites, pipes and unnatural cavity will affect the hydrogeology. Furthermore, local smaller fraction zones in the bedrock or soil layers can have large impact on the GW but are hard to capture in a larger scale investigation of the hydrogeology. These parameters are the most likely to have caused the misfit between simulated and observed head. The MODFLOW model doesn't account for land use, and it is assumed that every part of the studied area contributed equally to GW recharge.

The most probable refinement involves altering the calibration of the steady-state calculation, calibrated to maintain consistent flow through different layers compared to the base version calibrated with respect to a pumping test. This difference likely contributes to the deviations between the modelled and observed time series. Another potential factor could be uncertainties in the model stratigraphy, where discrepancies arise between the model representation and the actual soil and rock conditions on-site.

Another potential factor contributing to model discrepancies is the inability of the modelling software to account for negative recharge values. Negative recharge values imply water leaving the system rather than entering it, which could impact GW levels. As the model cannot compute negative values, they were excluded and replaced with zeros, potentially influencing model outcomes, although the exact impact remains uncertain. A possible solution to account for the negative recharge is the MODFLOW package UZF that could be implemented. Although further research needs to be put into investigating the efficacy of the UZF package.

The benchmark model could be further developed by adding additional stresses that can occur in an urban environment. There are several stresses that can be added such as leakage from drinking and wastewater system that occur in urban areas. When additional stresses can be added in the benchmark model to produce more developed timeseries that can be further used in timeseries modelling. By incorporating more stresses to the system, the evaluation of sensitivity and sources of interference can be evaluated in a larger scale.

For the period when the tunnel is being constructed the correlation between simulated and observed head are lower. This is most likely due to more disturbances in the soil and bedrock from the construction work that is not picked up in the calibration of the model. This will mean

that the model calibrated here can´t be used to extract accurate prediction of the site's hydrogeology. It can still give rough estimations and predictions from the start which can be helpful in planning the constructions. During the construction more data and investigations will lead to more understanding of the hydrogeology of the site. This knowledge can be used to improve the model during the construction period and can contribute to more precise estimations and predictions regarding the tunnel and its effects on the surroundings.

Before commencing the modelling using Pastas, it was established that comparing the groundwater flow model's accuracy involved comparing the raw output from MODEFLOW to the observed values. From the initial model iteration, it became evident that manually calibrating the model was an instructive albeit time-consuming process. The iterative process was presented in chapter 4.1 MODFLOW 2017-2019 are only a selection of the most significant model results and do not fully represent the extensive manual calibration process, which involved numerous iterations to achieve the results presented. The manual calibration could create the basis for a sensitivity analysis as the manual calibration process gave valuable insights toward which parameters affected the model results the most. However, manual calibration of a model of this scale is not recommended, and instead, automated calibration implementations such as PEST should be considered in the finalizing phase of the calibration. PEST is a software package capable of automatically calibrating parameters by testing combinations of values within user-defined ranges (USGS, 2022c). The reason why PEST calibration wasn't implemented was due to time constraints, and where further research should be put into implementing PEST calibration to improve the benchmark model with regard to representing the behaviour of the real hydrogeological system.

5.2 Time Series Modelling of Synthetic impacted groundwater heads

The Pastas models which have been used in this paper consistently showed good model fit, and the model fit did improve significantly by adding more stress data. The increase in model accuracy gained by adding stress data was expected given the definition of a TFN model.

By adding the calibration period to the Pastas models using synthetic head data, the model wasn't prone to overfitting the data thus yielding more representative results. The Pastas model with the leakage stress added consistently showed a correlation between 97-98 percent. The results from the Pastas models with leakage data added implies that there is not much more accuracy to be gained by adding more stresses since the correlation was with leakage data was good. Despite getting a good model fit by only adding the synthetic leakage to the pastas model it is still of interest to build upon this model by adding additional stresses to the model.

For the observation well HH4297B which did have measured data the model fit was good, despite not adding any external stresses. By adding more stresses, the model fit would have likely improved, however this was not possible since not data for any additional stresses was available.

The results from the Pastas modelling shows that the MODFLOW model can be used as a benchmark model as the GW time series from MODFLOW could be used to create a functioning Pastas Model. Due to time constraints and how the MODFLOW model was built it was not possible to retrieve more synthetic stresses to add to the Pastas model. But further research should be put into retrieving more synthetic stresses to thoroughly test TFN models for estimating groundwater impacts.

6
Conclusions

The benchmark model was calibrated iteratively by adjusting parameters such as hydraulic conductivity, specific yield, and specific storage to simulate groundwater leakage to a tunnel accurately. Despite this calibration, discrepancies remained between simulated and observed data, necessitating further modifications, including a 1-meter adjustment to the observed head data to align trends over time. Simulated time series from the benchmark model demonstrated a high correlation with observed data, particularly when accounting for tunnel-induced drawdown, highlighting the model's utility in estimating leakage effects. The synthetic leakage calculated from the benchmark model was used as input for the TFN model, which showed improved fit and capability in representing groundwater drawdown due to tunnel construction. The results indicate that while synthetic data provided a reliable estimate, using measured data where available further enhanced the accuracy and correlation of the time series model.

6.1 Suggestions for future research

Given the limitations discussed in this thesis, several recommendations are proposed to address these gaps and enhance the accuracy of the methodology. These recommendations are as follows:

- Future studies could benefit from more comprehensive and continuous data collection efforts, minimizing gaps and reducing the need for data adjustments and interpolation.
- Enhanced Model Calibration: Increasing the number of observation wells and extending the monitoring period could improve model calibration and the robustness of the correlations between observed and simulated data. Where PEST calibration is an example of such enhanced model calibration tool
- Advanced Modelling Techniques: Incorporating more sophisticated models that can better capture the complexities of evapotranspiration, recharge processes, and tunnel leakage could enhance the accuracy of predictions.
- Consideration of Long-term Impacts: Extending the analysis to cover longer time periods could provide insights into the long-term impacts of tunnel construction on GW systems.

Bibliography

Bakker, M. (2019). *Time Series Analysis to the Rescue.* Groundwater.

Bakker, M., & Schaars, F. (2019). Solving Groundwater Flow Problems with Time Series Analysis: You May Not Even Need Another Model. *Ground Water*.

Barthel, R., Haaf, E., Nygren, M., & Giese, M. (2022). Systematic visual analysis of groundwater hydrographs: potential benefits and challenges. *Hydrogeology Journal*.

Boström, L., & Lindblom, A. (2021). *Evaluatin transfer-function models to understand groundwater level impacts.* Göteborg: Chalmers University of Technology.

Collenteur, R. (2019). Pastas: Open Source Software for the Analysis of Groundwater Time Series. *Groundwater*.

Feijóo, A., & Villanueva, D. (2016). *Assessing wind speed simulation methods.* Renewable and Sustainable Energy Reviews.

Florén, S. (2015). *Grundvattenbildning till berg.* Lund: Lunds Universitet.

Haaf, E., Giese, M., Reimann, T., & Barthel, R. (2023). *Data-Driven Estimation of Groundwater Level Time-Series at Unmonitored Sites Using Comparative Regional Analysis.* Water Resources Research.

Law, M., & Jackson, D. (2017). Residual plots for linear regression models with censored outcome data: A refined method for visualizing residual uncertainty. *Communications in Statistics - Simulation and Computation*.

Lu, M., Rogiers, B., Beerten, K., Gedegon, M., & Huysmans, M. (2022). Exploring river–aquifer interactions and hydrological system response using baseflow separation, impulse response modeling, and time series analysis in three temperate lowland catchments. *Hydrology and earth system sciences*.

Luetkemeier, R., Söller, L., & Frick-Trzebitzky, F. (2022). Anthropogenic Pressures on Groundwater. *Encyclopedia of Inland Waters (Second Edition)*.

MathWorks. (n.d). *What is convolution?* Retrieved from https://se.mathworks.com/discovery/convolution.html

Olofsson, B., Jacks, G., Knutsson, G., & Thunvik, R. (2001). Grundvatten i hårt berg - en analys av kunskapsläget. In *Kunskapsläget på kärnavfallsområdet 2001* (pp. 113-371). Stockholm: KASAM.

Pezij, M., Augustijn, D. C., Hendriks, D. M., & Hulscher, S. J. (2020). Applying transfer function-noise modelling to characterize soil moisture dynamics: a data-driven approach using remote sensing data. *Environmental Modelling & Software*.

Pool, M., Sterte-Jutebring, E., Ploum, S., Lindborg, E., Claesson Liljedahl, L., Haaf, E., . . . Sundell, J. (2024). *GROUNDWATER LEVELS OF OPEN BOREHOLES IN BEDROCK VS MODELLING RESULTS.* BeFo Rapport (in press).

Rutgersson, A., Omstedt, A., & Räisänen, J. (2002). *Net precipitation over the Baltic Sea during present and future climate conditions.* Norrköping: Inter-Research Science Publisher.

SGU. (2019). *Hydrogeologiska förutsättningar*. Retrieved from sgu.se: https://www.sgu.se/anvandarstod-for-geologiska-fragor/bedomning-av-influensomrade-avseende-grundvatten/utgangslage-och-utredningsstrategi/hydrogeologiska-forutsattningar/

SGU. (2020a). *The bedrock of Sweden*. Retrieved from sgu.se: https://www.sgu.se/en/geology-of-sweden/rocks/the-bedrock-of-sweden/

SGU. (2020b). *Glaciala finkorniga sediment*. Retrieved from https://www.sgu.se/om-geologi/jord/fran-istid-till-nutid/isen-smalter/glaciala-finkorniga-sediment/

SGU. (2020c). *Morän – spår av inlandsisen*. Retrieved from https://www.sgu.se/om-geologi/jord/fran-istid-till-nutid/inlandsisen/moran-spar-av-inlandsisen/
SGU. (2023). *Berggrund 1:50 000 - 1:250 000*. Retrieved from https://www.sgu.se/produkter-och-tjanster/kartor/kartvisaren/bergkartvisare/berggrund-150-000-1250-000/
Shen, S.-L., & Xu, Y. (2006). Analysis of Settlement Due to Withdrawal of Groundwater Around an Unexcavated Foundation Pit. *Geotechnical Special Publication*.
SMHI. (n.d). *Ladda ner meteorologiska observationer*. Retrieved from smhi.se: https://www.smhi.se/data/meteorologi/ladda-ner-meteorologiska-observationer/#param=precipitation24HourSum,stations=core
Spross, J. (2009). *Mätning av inläckande vatten i bergtunnlarna inom projekt Norra länken.* Trafikverket.
Sundell, J., Norberg, T., Haaf, E., & Rosén, L. (2019). *Economic valuation of hydrogeological information when managing groundwater drawdown.* Hydrogeology Journal.
Sundkvist, U. (2016). *PM Hydrogeologiska beräkningar.* Trafikverket.
Trafikverket. (2013). *Olskroken planskildhet och Västlänken, Underlagsrapport Geologi och hydrogeologi.* Göteborg: Trafikverket.
Trafikverket. (2020). *Informationsmaterial – deletapp Haga.*
Trafikverket. (2022). *Västlänken*. Retrieved from https://www.trafikverket.se/: https://www.trafikverket.se/vara-projekt/projekt-i-vastra-gotalands-lan/vastlanken/
USGS. (2003). *Understanding the Principles of Groundwater.*
USGS. (2020). *Hydrogeology and groundwater geochemistry of till confining units and confined aquifers in glacial deposits near Litchfield, Cromwell, Akeley, and Olivia, Minnesota, 2014–18.*
USGS. (2021). *ModelMuse: A Graphical User Interface for Groundwater Models*. Retrieved from https://www.usgs.gov/: https://www.usgs.gov/software/modelmuse-a-graphical-user-interface-groundwater-models
USGS. (2022a). *MODFLOW and Related Programs*. Retrieved from https://www.usgs.gov/mission-areas/water-resources/science/modflow-and-related-programs
USGS. (2022b). *MODFLOW-NWT: A Newton Formulation for MODFLOW-2005*. Retrieved from https://www.usgs.gov/: https://www.usgs.gov/software/modflow-nwt-a-newton-formulation-modflow-2005
USGS. (2022c). *Working with PEST*. Retrieved from https://water.usgs.gov/nrp/gwsoftware/ModelMuse/Help/working_with_pest.html
USGS. (n.d). *What is the difference between a confined and an unconfined (water table) aquifer?* Retrieved from https://www.usgs.gov/faqs/what-difference-between-a-confined-and-unconfined-water-table-aquifer
von Asmuth, J., Bierkens, M., & Maas, K. (2002, December 11). Transfer function-noise modeling in continuous time using predefined impulse response functions. *Water Resources Research*. Retrieved from https://agupubs.onlinelibrary.wiley.com/doi/10.1029/2001WR001136
Vremec, M. (2022). Technical note: Improved handling of potential evapotranspiration in hydrological studies with PyEt. *Hydrology and Earth System Sciences*.
Vägverket. (2000). *Tätning av bergtunnlar –förutsättningar, bedömningsgrunder och strategi vid planering och utformning av tätningsinsatser.*

Woessner, W., & Poeter, E. (2020). Specific Yield and Specific Retention. In W. W. Woessner, & E. P. Poeter, *Hydrogeologic Properties of Earth Material and Principles of Groundwater Flow.* Ontario, Canada: The Groundwater Project.

Yoo, C. (2016). Ground settlement during tunneling in groundwater drawdown environment – Influencing factors. *Underground Space*.

Appendix

Appendix 1: Python code for PyEt calculations

```
import pandas as pd
import pyet
import numpy
import pyet
import os

# Create an empty DataFrame to store the potential evapotranspiration (PE) results for different methods
pet_results = pd.DataFrame()


# Data needing processing
# wind data
wind=pd.read_excel("Insert your file path", index_col=0, parse_dates=True)
wind=wind.groupby(pd.Grouper(freq='24H')).mean().round(1)
wind.rename(columns={wind.columns[0]: 'wind'}, inplace=True)
#print(wind)

# Rh data
rh = pd.read_excel(r"Insert ", index_col=0, parse_dates=True)
rh=rh.groupby(pd.Grouper(freq='24H')).mean().round(1)
rh.rename(columns={rh.columns[0]: 'rh'}, inplace=True)


# Data ready to read
# temp data
temp_mean=pd.read_excel("Insert your file path", index_col=0, parse_dates=True)
temp_mean.rename(columns={temp_mean.columns[0]: 'tmean'}, inplace=True)

temp_min=pd.read_excel("Insert your file path", index_col=0, parse_dates=True)
temp_min.rename(columns={temp_min.columns[0]:'tmin'}, inplace=True)

temp_max=pd.read_excel("Insert your file path", index_col=0, parse_dates=True)
temp_max.rename(columns={temp_max.columns[0]:'tmax'}, inplace=True)

#rs data
rs = pd.read_excel("Insert your file path", index_col=0, parse_dates=True)
rs.rename(columns={rs.columns[0]: 'rs'}, inplace=True)

# Define the latitude and elevation separately as single values
lat_value = XXXX #hight above sealevel weather station
lat = float(lat_value) * numpy.pi / 180
elevation_value = XXXX #latitude weather station
elevation = float(elevation_value)

# Combine all datasets into one DataFrame, aligning them based on datetime index
combined_data = pd.concat([temp_mean, wind, rs, rh, temp_max, temp_min], axis=1, join="outer")

# Calculate Potential Evapotranspiration (PE) using pyet
pet_results = pyet.calculate_all(tmean=combined_data["tmean"], wind=combined_data["wind"],
                        rs=combined_data["rs"], elevation=elevation,
                        lat=lat, tmax=combined_data["tmax"],
                        tmin=combined_data["tmin"], rh=combined_data["rh"])



# Reset index setting
pet_results = pet_results.reset_index()

# Save the PET DataFrame to a xlsx file
# Input name of original file
```

```
original_file_name = 'Insert your prefered file name'

# Create a directory to store the output file
output_dir = "Insert your file path"
if not os.path.exists(output_dir):
    os.makedirs(output_dir)

# Generate the file name for the new Excel file
base_file_name = os.path.basename(original_file_name)
new_file_name = 'Insert your prefered file name' + base_file_name + '.xlsx'
file_path = os.path.join(output_dir, new_file_name)

# Export DataFrame to Excel
try:
    pet_results.to_excel(file_path, index=False)
    print(f"Data successfully exported to {file_path}")
except Exception as e:
    print(f"Error exporting data: {e}")

```

Appendix 1: PyEt Example Code

Appendix 2: Python code for Pastas model without leakage

```
import pandas as pd
import pastas as ps
import numpy as np
import matplotlib.pyplot as plt
import math

# Import pandas library
import pandas as pd

# Import climate data
Climatedata = pd.read_excel("Insert your file path")

# Set 'Unnamed: 0' as the index column and rename it to 'Date'
Climatedata.set_index('Representativt dygn', inplace=True)
Climatedata.index.name = 'Datum'

# Extract columns
Precipitation = Climatedata['Nederbördsmängd']
Evapotranspiration = Climatedata['Penman']
Recharge = Climatedata['Recharge']

# Create DataFrames
Prec = pd.DataFrame(Precipitation, columns=['Nederbördsmängd'])
Evap = pd.DataFrame(Evapotranspiration, columns=['Penman'])
Rech = pd.DataFrame(Recharge, columns=['Recharge'])

#Replacing the Negative values with Zeroes

# Define a function to replace negative values with zero
def replace_negatives_with_zero(x):
    if x < 0:
        return 0
    else:
        return x

# Apply the function to each element of the 'Recharge' column
RechAmended = pd.DataFrame(Recharge.apply(replace_negatives_with_zero), columns=['Recharge'])

# Display the new DataFrame

#import Simulated values
# Read the Excel file into a DataFrame
df = pd.read_excel(" Insert your file path ")

# Extract the well name without the index
df["WELL_NAME"] = df["\"OBSERVATION NAME\""].str.extract(r'(HH\d+[A-Z]+)')

# Group the data by "WELL_NAME"
grouped = df.groupby("WELL_NAME")

# Create a dictionary to store the separate DataFrames for each well
well_dataframes = {}

# Iterate over groups and create separate DataFrames
for name, group in grouped:
    well_dataframes[name] = group.copy()

    # Remove the suffix from the "WELL_NAME" column
    well_dataframes[name]["WELL_NAME"] = name

# For HH40031
Simulated_HH4001H = well_dataframes["HH4001H"]
Simulated_HH4001H.set_index('Unnamed: 0', inplace=True)
Simulated_HH4001H = Simulated_HH4001H.drop(columns=["\"OBSERVED VALUE\"", "\"OBSERVATION NAME\"",
"WELL_NAME"])

```

```
#import Observed values
MeasuredValues=pd.read_excel(" Insert your file path")

Measured_HH4297B = MeasuredValues[['Date', 'Stress period', 'HH4297B']]
Measured_HH4297B = Measured_HH4297B.drop(columns=["Stress period"])
Measured_HH4297B.set_index('Date', inplace=True)

# Convert the index to a DatetimeIndex with a specified frequency
Simulated_HH4001H.index = pd.to_datetime(Simulated_HH4001H.index, errors='coerce', format='%Y-%m-%d %H:%M:%S')

# Remove spaces from column names
Simulated_HH4001H.columns = [col.replace(' ', '') for col in Simulated_HH4001H.columns]
```

```
# Create the pastas Model (Simulated
SimulatedModelHH40001H = ps.Model(Simulated_HH4001H)
SMHH4001H = ps.RechargeModel(prec=Prec, evap=Evap, rfunc=ps.Gamma())
SimulatedModelHH40001H.add_stressmodel(SMHH4001H)
SimulatedModelHH40001H.solve(tmin="2021", tmax="2023", noise=False)
SimulatedModelHH40001H.plots.results()
```

```
Measured_HH4302U.index = pd.to_datetime(Measured_HH4302U.index, errors='coerce', format='%Y-%m-%d %H:%M:%S')

# Remove spaces from column names
Measured_HH4302U.columns = [col.replace(' ', '') for col in Measured_HH4302U.columns]

# Create the pastas Model
SimulatedModelMeasured_HH40003H = ps.Model(Measured_HH4302U)
SMMeasured_HH40003H = ps.RechargeModel(prec=Prec, evap=Evap, rfunc=ps.Gamma())
SimulatedModelMeasured_HH40003H.add_stressmodel(SMMeasured_HH40003H)
SimulatedModelMeasured_HH40003H.solve(tmin="2021", tmax="2023", noise=False)
SimulatedModelMeasured_HH40003H.plots.results()

```

Appendix 2: Base Pastas model used.

Appendix 3: Python code for Calibrated model

```
import pastas as ps
import pandas as pd
import matplotlib.pyplot as plt
import math

#import Simulated values
# Read the Excel file into a DataFrame
df = pd.read_excel(r"C:\Users\A546455\Exjobb\Brunnsdata -Efter Tunnelstart\HOB_20-23_Pastas.xlsx")

# Extract the well name without the index
df["WELL_NAME"] = df["\"OBSERVATION NAME\""].str.extract(r'(HH\d+[A-Z]+)')

# Group the data by "WELL_NAME"
grouped = df.groupby("WELL_NAME")

# Create a dictionary to store the separate DataFrames for each well
well_dataframes = {}

# Iterate over groups and create separate DataFrames
for name, group in grouped:
    well_dataframes[name] = group.copy()

    # Remove the suffix from the "WELL_NAME" column
    well_dataframes[name]["WELL_NAME"] = name

# For HH4107U
Simulated_HH4107U = well_dataframes["HH4107U"]
Simulated_HH4107U.set_index('Unnamed: 0', inplace=True)
Simulated_HH4107U = Simulated_HH4107U.drop(columns=["\"OBSERVED VALUE\"", "\"OBSERVATION NAME\"", "WELL_NAME"])

# Import climate data
Climatedata = pd.read_excel(r"C:\Users\A546455\Exjobb\Brunnsdata -Efter Tunnelstart\weekly_data_Recharge_Pastas.xlsx")

# Set 'Unnamed: 0' as the index column and rename it to 'Date'
Climatedata.set_index('Representativt dygn', inplace=True)
Climatedata.index.name = 'Datum'

# Extract columns
Precipitation = Climatedata['Nederbördsmängd']
Evapotranspiration = Climatedata['Penman']
Recharge = Climatedata['Recharge']

# Create DataFrames
Prec = pd.DataFrame(Precipitation, columns=['Nederbördsmängd'])
Evap = pd.DataFrame(Evapotranspiration, columns=['Penman'])
Rech = pd.DataFrame(Recharge, columns=['Recharge'])

# Define a function to replace negative values with zero
def replace_negatives_with_zero(x):
    if x < 0:
        return 0
    else:
        return x

# Apply the function to each element of the 'Recharge' column
RechAmended = pd.DataFrame(Recharge.apply(replace_negatives_with_zero), columns=['Recharge'])

ExtractedLeakage=pd.read_excel(r"C:\Users\A546455\Exjobb\Brunnsdata -Efter Tunnelstart\Läckage.xlsx")
ExtractedLeakage.set_index('Date', inplace=True)
ExtractedLeakage = ExtractedLeakage.drop(columns=["Utan tunnel"])
ExtractedLeakage = ExtractedLeakage.drop(columns=["Med tunnel"])
ExtractedLeakage = ExtractedLeakage.drop(columns=["Läckage"])
```

```
ExtractedLeakage=pd.DataFrame(ExtractedLeakage,columns=['Leakage'])
print(ExtractedLeakage)

CoordRef=[147744,6397696]
Coord4001=[147758,6397833]
Coord4003=[147812,6397486]
Coord4107=[147969,6397662]
Coord4297=[147880,6397718]
Coord4302=[147889,6397694]


Ref_4001= math.sqrt(((CoordRef[0] - Coord4001[0]) ** 2) + ((CoordRef[1] - Coord4001[1]) ** 2))
Ref_4003= math.sqrt(((CoordRef[0] - Coord4003[0]) ** 2) + ((CoordRef[1] - Coord4003[1]) ** 2))
Ref_4107= math.sqrt(((CoordRef[0] - Coord4107[0]) ** 2) + ((CoordRef[1] - Coord4107[1]) ** 2))
Ref_4297= math.sqrt(((CoordRef[0] - Coord4297[0]) ** 2) + ((CoordRef[1] - Coord4297[1]) ** 2))
Ref_4302= math.sqrt(((CoordRef[0] - Coord4302[0]) ** 2) + ((CoordRef[1] - Coord4302[1]) ** 2))

Distances = [Ref_4001, Ref_4003, Ref_4107, Ref_4297, Ref_4302]
Leakage = [ExtractedLeakage, ExtractedLeakage, ExtractedLeakage, ExtractedLeakage, ExtractedLeakage]

# Create the Pastas model using the training data
ml = ps.Model(Simulated_HH4107U)

# Example of adding a Linear Recharge Model

Rch=ps.rch.Linear()
sm_linear = ps.RechargeModel(prec=Prec, evap=Evap, rfunc=ps.Exponential(), recharge=Rch,name='linear_recharge')
ml.add_stressmodel(sm_linear)

leak = ps.WellModel(Leakage, rfunc=ps.HantushWellModel(), name="leakage", distances=Distances, settings="well")
ml.add_stressmodel(leak)

# Train the model using the training data
ml.solve()


```

Appendix 3: Example code of a calibrated Pastas model

Appendix 4: Python code for resampling to weekly data

```
SP=r"Insert your file path"
DF=pd.read_excel(SP)
filtered_data = DF.loc[DF['Benämning'] == 'HH4297B', ['Tidpunkt', 'Värde']]

# Set 'Tidpunkt' column as the index
filtered_data.set_index('Tidpunkt', inplace=True)

# Resample the data by weekly intervals and calculate the mean for each week
weekly_data = filtered_data.resample('W').mean()

# Display the weekly data
weekly_data=weekly_data.loc['2017-09-24':'2019-09-30']
weekly_data.to_excel('weekly_data.xlsx')
weekly_data.to_excel('Insert your file path')

SP=r"Insert your file path"
```

```
df=pd.read_excel(SP)
df['Representativt dygn'] = pd.to_datetime(df['Representativt dygn'])

# Set 'Representativt dygn' column as the index
df.set_index('Representativt dygn', inplace=True)

# Resample the data by weekly intervals and calculate the sum for each week
weekly_data = df.resample('w').sum()  # Change 'sum' to any aggregation function you desire

# Display the weekly data
print(weekly_data)
weekly_data=weekly_data.loc['2015-10-01':'2017-09-24']
weekly_data.to_excel('weekly_data.xlsx')
weekly_data.to_excel('Insert your file path')

SP=r"Insert your file path"
df=pd.read_excel(SP)
df['index'] = pd.to_datetime(df['index'])

# Set 'Representativt dygn' column as the index
df.set_index('index', inplace=True)

# Resample the data by weekly intervals and calculate the sum for each week
weekly_data = df.resample('W').sum()  # Change 'sum' to any aggregation function you desire

# Display the weekly data
print(weekly_data)
weekly_data=weekly_data.loc['2015-10-01':'2017-09-24']
weekly_data.to_excel('weekly_data.xlsx')
weekly_data.to_excel(r'Insert your search path')

# Load the first DataFrame
SP = r"Insert your search path"
df = pd.read_excel(SP)

# Load the second DataFrame
SP2 = r"Insert your search path"
df2 = pd.read_excel(SP2)

# Set 'Representativt dygn' column as the index for both DataFrames
df.set_index(df.columns[0], inplace=True)
df2.set_index(df2.columns[0], inplace=True)

# Merge the two DataFrames based on the index column (dates)
merged_df = pd.merge(df, df2, left_index=True, right_index=True, suffixes=('', '_right'))

# Drop the 'index' column
merged_df['Recharge'] = merged_df['Nederbördsmängd'] - merged_df['Penman']

merged_df=merged_df.loc['2015-10-01':'2017-09-24']
# Display the updated DataFrame
print(merged_df)

merged_df.to_excel('weekly_data.xlsx')
merged_df.to_excel(r'Insert your search path')

```

Appendix 4: Resampling code

Appendix 5: Python code for plotting results

```
import pandas as pd
import matplotlib.pyplot as plt

# Simulated welldata from 21-23_Kmean_D30
df = pd.read_excel(r"Insert your search path")
df=df.drop(columns=['"OBSERVED VALUE"'])
df=df.drop(columns=['Unnamed: 0'])
# Replace the name HH4107U_x with HH4107U
df['"OBSERVATION NAME"'] = df['"OBSERVATION NAME"'].str.replace(r'(HH4107U)_\d+', r'\1')
```

```
df["'OBSERVATION NAME"'] = df["'OBSERVATION NAME"'].str.replace(r'(HH4302U)_\d+', r'\1')
df["'OBSERVATION NAME"'] = df["'OBSERVATION NAME"'].str.replace(r'(HH4297B)_\d+', r'\1')
df["'OBSERVATION NAME"'] = df["'OBSERVATION NAME"'].str.replace(r'(HH4001H)_\d+', r'\1')
df["'OBSERVATION NAME"'] = df["'OBSERVATION NAME"'].str.replace(r'(HH4003H)_\d+', r'\1')
# Extract the well name without the index
df["WELL_NAME"] = df["'OBSERVATION NAME"']
# Group the data by "WELL_NAME"
grouped = df.groupby("WELL_NAME")
# Create a dictionary to store the separate DataFrames for each well
well_dataframes = {}
# Iterate over groups and create separate DataFrames
for name, group in grouped:
    well_dataframes[name] = group.drop(columns=["WELL_NAME"])
    #print(name)  # Add this line to print the keys
# Access the well dataframes
Simulated_HH4001H = well_dataframes["HH4001H"]
Simulated_HH4001H = Simulated_HH4001H.drop(columns=["'OBSERVATION NAME"'])
Simulated_HH4001H.reset_index(drop=True, inplace=True)
HH4001H_Kmean_D30=Simulated_HH4001H
Simulated_HH4003H = well_dataframes["HH4003H"]
Simulated_HH4003H = Simulated_HH4003H.drop(columns=["'OBSERVATION NAME"'])
Simulated_HH4003H.reset_index(drop=True, inplace=True)
HH4003H_Kmean_D30=Simulated_HH4003H
Simulated_HH4297B = well_dataframes["HH4297B"]
Simulated_HH4297B = Simulated_HH4297B.drop(columns=["'OBSERVATION NAME"'])
Simulated_HH4297B.reset_index(drop=True, inplace=True)
HH4297B_Kmean_D30=Simulated_HH4297B
Simulated_HH4107U = well_dataframes["HH4107U"]
Simulated_HH4107U = Simulated_HH4107U.drop(columns=["'OBSERVATION NAME"'])
Simulated_HH4107U.reset_index(drop=True, inplace=True)
HH4107U_Kmean_D30=Simulated_HH4107U
Simulated_HH4302U = well_dataframes["HH4302U"]
Simulated_HH4302U = Simulated_HH4302U.drop(columns=["'OBSERVATION NAME"'])
Simulated_HH4302U.reset_index(drop=True, inplace=True)
HH4302U_Kmean_D30=Simulated_HH4302U

# Import recharge data
Recharge = pd.read_excel(r"Insert your search path")

# Drop the first four columns
Recharge.drop(Recharge.columns[:4], axis=1, inplace=True)

# Replace negative values with 0
Recharge = Recharge.applymap(lambda x: 0 if x < 0 else x)

# Plot the data
ax = Recharge.plot(figsize=(12, 4))

# Customize the plot
plt.xticks(range(0, len(Recharge), 5))
plt.grid(True)
plt.ylabel('Precipitation [mm/year]')
plt.xlabel('Time [step]')
plt.title('Recharge')

# Change legend label
ax.legend(['Recharge'])









plt.show()



plt.figure(figsize=(12, 4))
plt.plot(Kmean_D30[start_index:], label='Simulated head', color='black')
plt.scatter(range(start_index, end_index), Obs[start_index:],
```

```
            label='Observed head', color='red', marker='.')
plt.title(title[0]); plt.ylabel('Head [m]'); plt.xlabel('Time [step]');
plt.xticks(range(start_index, end_index, 5))
plt.legend(); plt.grid(True)
plt.savefig(r"Insert your search path")

#Plottar simulerade värden med observerade korrigerade värden
plt.figure(figsize=(12, 4))
plt.plot(Kmean_D30[start_index:], label='Simulated Head', color='black')
plt.scatter(range(start_index, end_index), Obs_K[start_index:],
            label='Modified Observed Head', color='magenta', marker='.')
plt.title(title[0]); plt.ylabel('Head [m]'); plt.xlabel('Time [step]');
plt.xticks(range(start_index, end_index, 5))
plt.legend(); plt.grid(True)
plt.savefig(r"Insert your search path")

#R-square
from sklearn.metrics import r2_score
# Interpolate both DataFrames
Simulated_Interpolated = Kmean_D30.interpolate()
Obs_Interpolated = Obs_K.interpolate()
# Extract the columns that you want to compare
y_true = Simulated_Interpolated['SIMULATED EQUIVALENT']
y_pred = Obs_Interpolated
# Drop NaN values from both y_true and y_pred
y_true = y_true.dropna()
y_pred = y_pred[y_pred.index.isin(y_true.index)]  # Only keep values in y_pred that correspond to non-NaN indices in y_true
# Compute the R-squared value
r_squared = r2_score(y_pred, y_true)

print("R-squared value:", r_squared)

```

Appendix 5: Code used to plot time series.

Appendix 6-8: Simulated and modified observed head 2017-2019

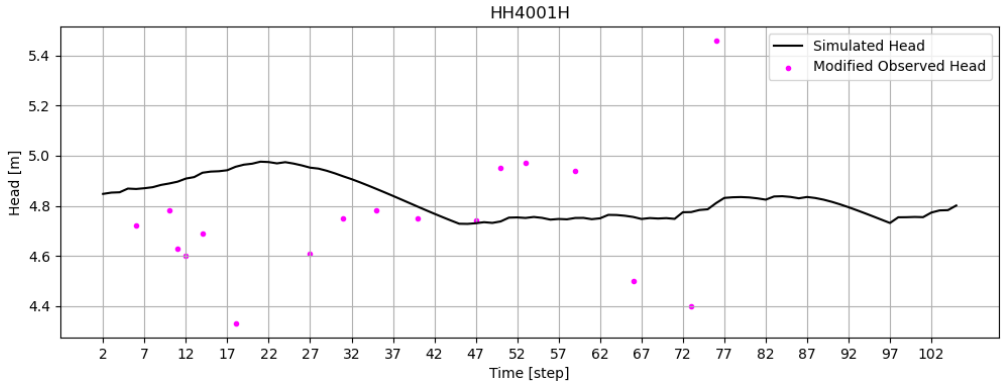

Appendix 6 Appendix: Simulated and modified observed head for HH4001H, 2017-2019.

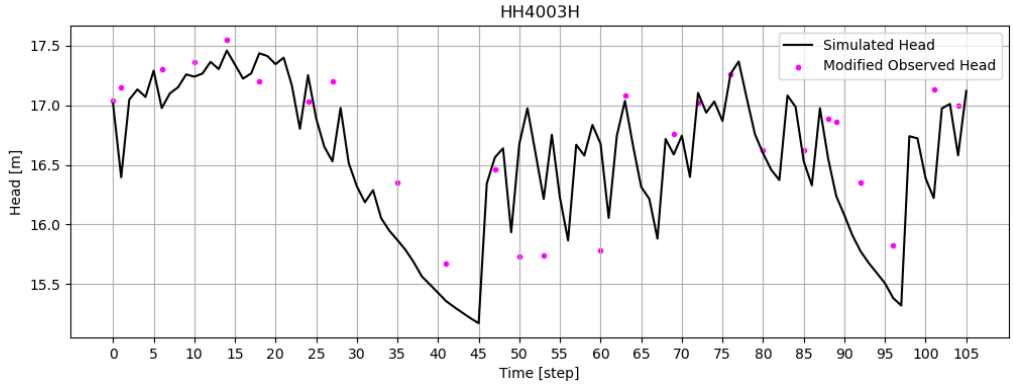

Appendix 7 Simulated and modified observed head for HH4003H, 2017-2019.

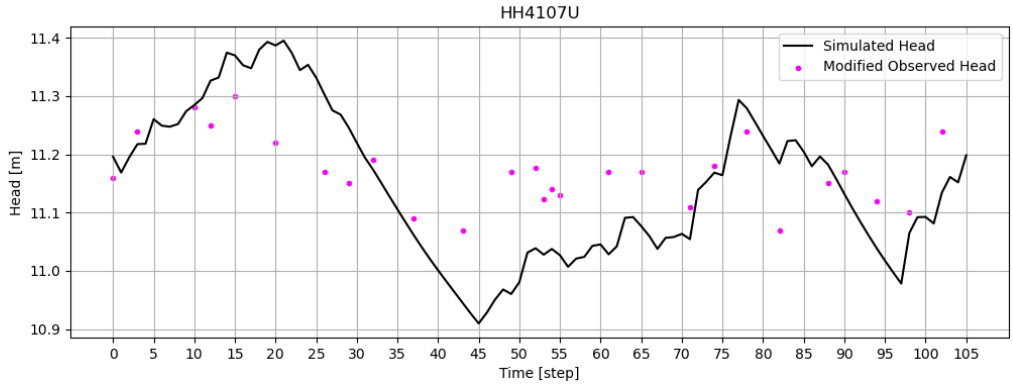

Appendix 8 Simulated and modified observed head for HH4107U, 2017-2019.

Appendix 9-11: Simulated and observed head 2021-2023

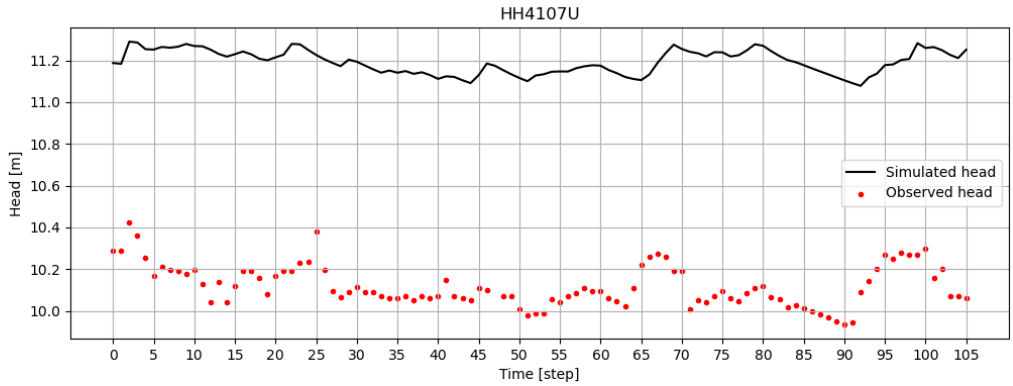

Appendix 9 Simulated and observed head for HH4107U, 2021-2023.

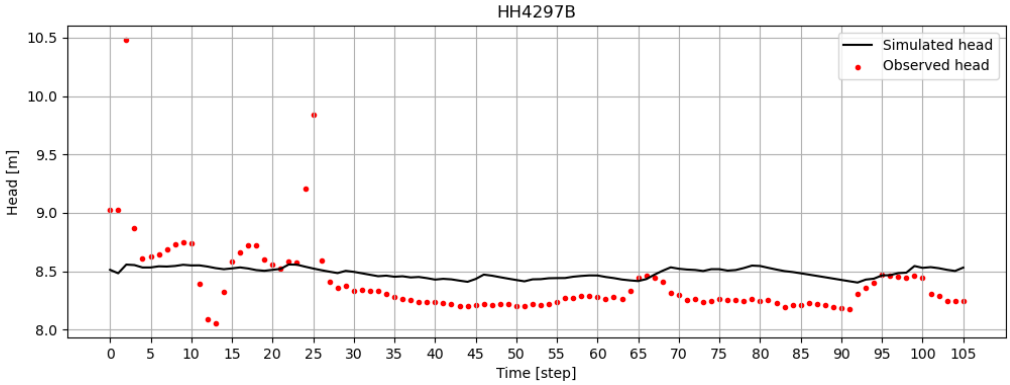

Appendix 10 Simulated and observed head for HH4297B, 2021-2023.

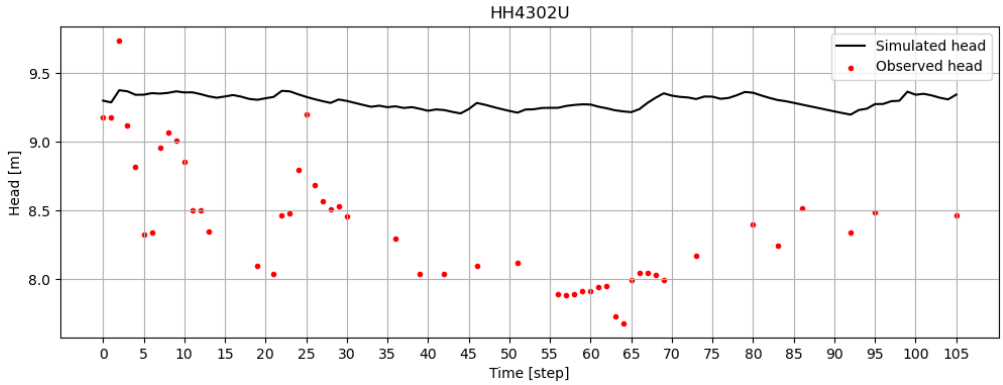

Appendix 11 Simulated and observed head for HH4302, 2021-2023.

Appendix 12-14: Simulated and modified observed head 2021-2023

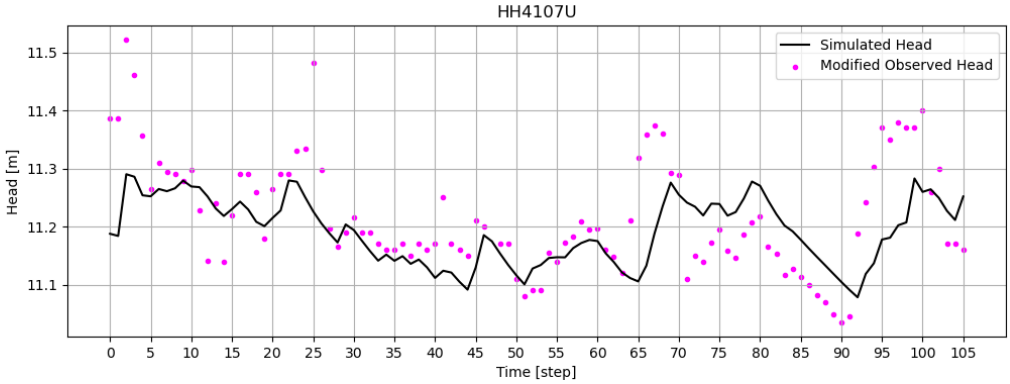

Appendix 12 Simulated and modified observed head for HH4107U, 2021-2023.

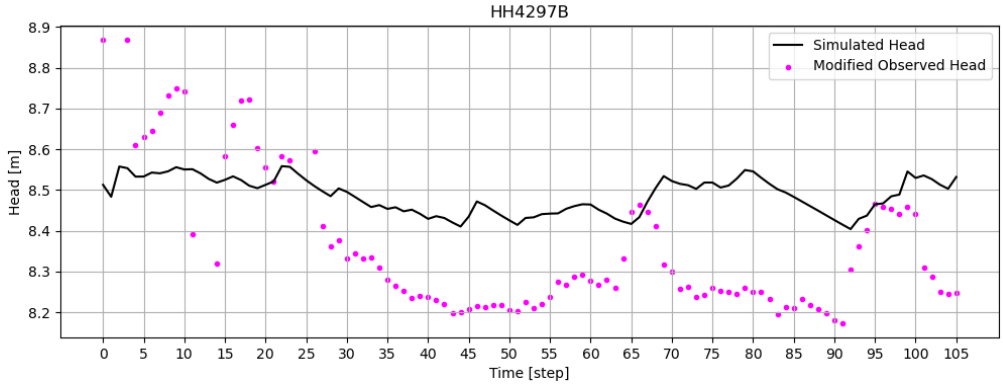

Appendix 13 Simulated and modified observed head for HH4297B, 2021-2023.

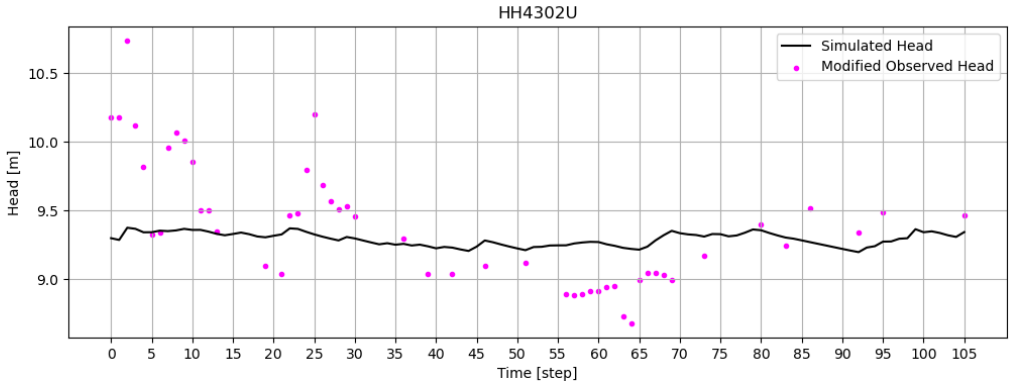

Appendix 14 Simulated and modified observed head for HH4302U, 2021-2023.

Appendix 15-19: Simulated head without and with a tunnel

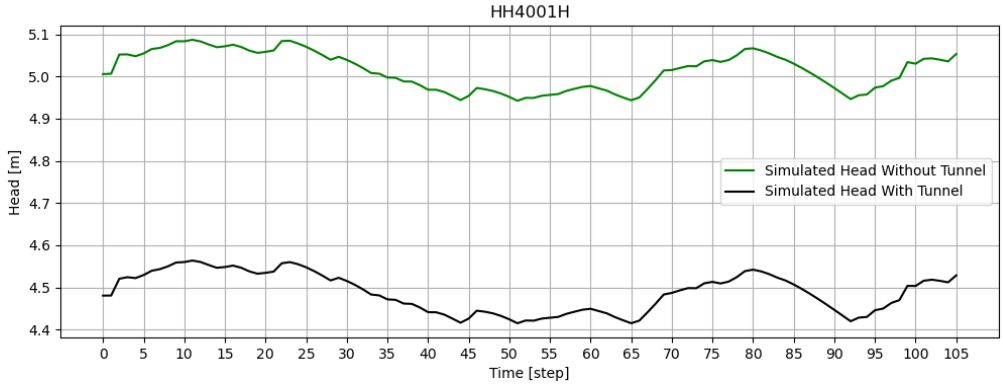

Appendix 15 Simulated head without and with a tunnel for HH4001H, 2021-2023.

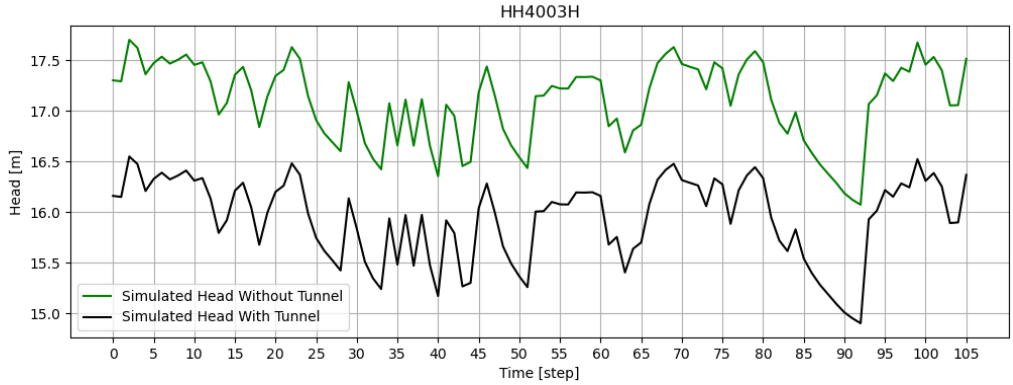

Appendix 16 Simulated head without and with a tunnel for HH4003H, 2021-2023.

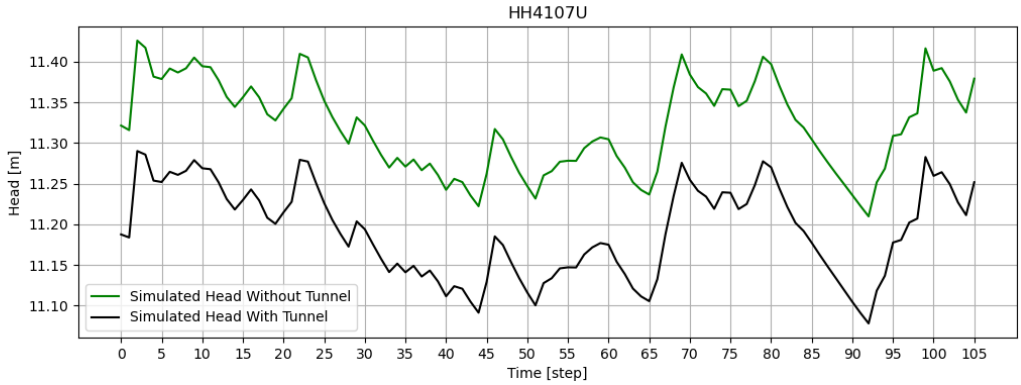

Appendix 17 Simulated head without and with a tunnel for HH4107U, 2021-2023.

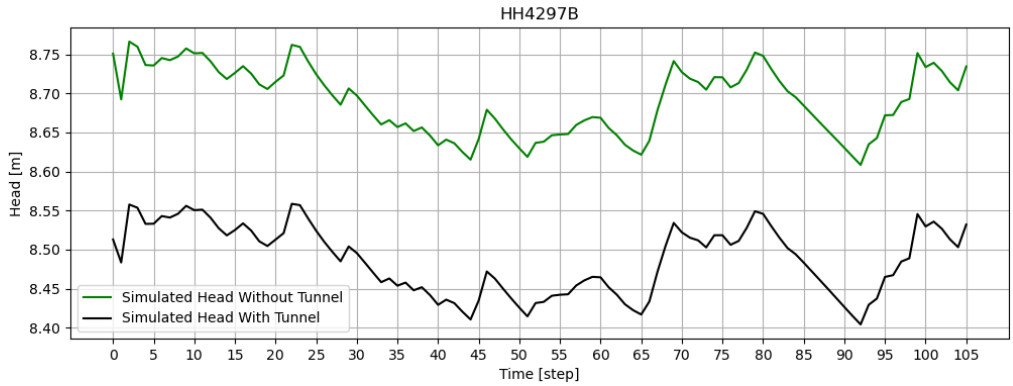

Appendix 18 Simulated head without and with a tunnel for HH4297B, 2021-2023.

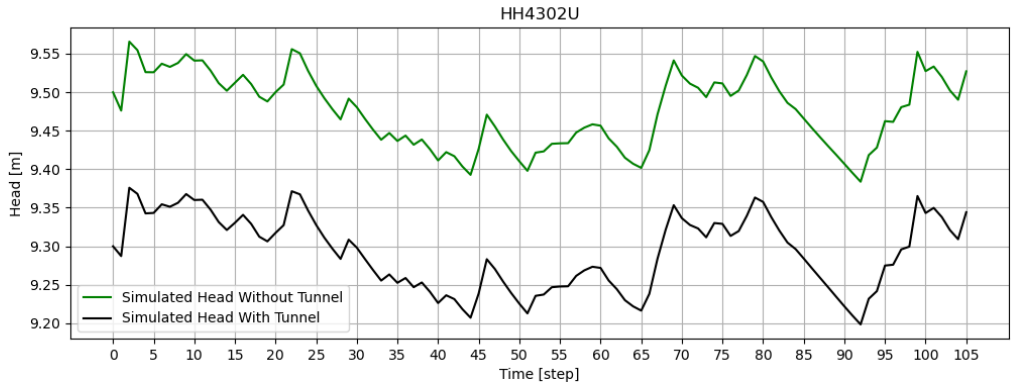

Appendix 19 Simulated head without and with a tunnel for HH4302U, 2021-2023.

Appendix 20-24: Simulated head for different conductivity

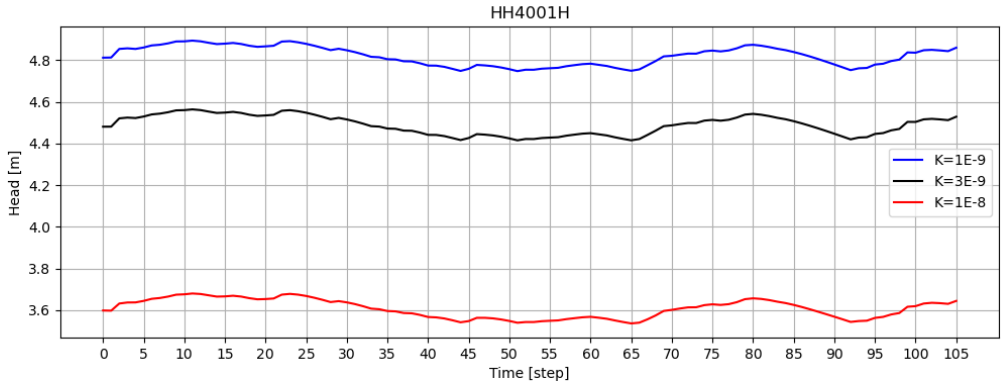

Appendix 20 Simulated head for different conductivity in the tunnel for HH4001H, 2021-2023.

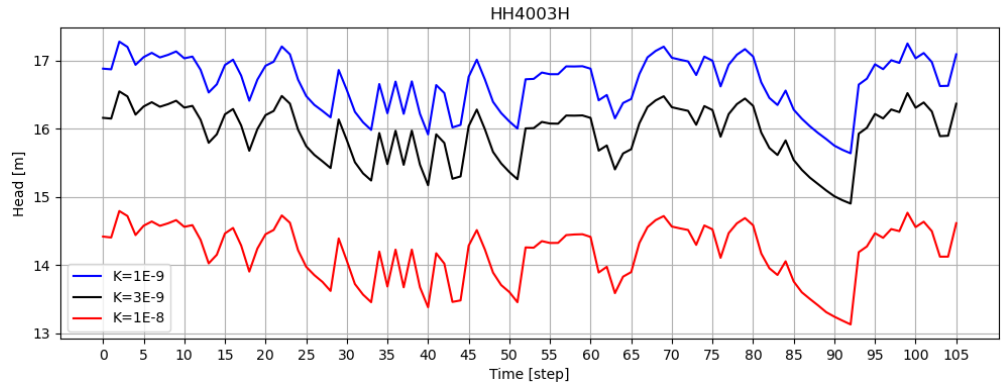

Appendix 21 Simulated head for different conductivity in the tunnel for HH4003H, 2021-2023.

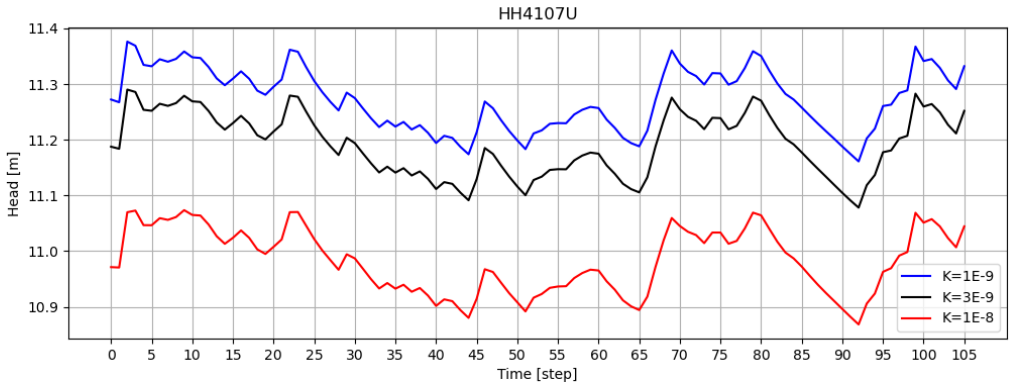

Appendix 22 Simulated head for different conductivity in the tunnel for HH4107U, 2021-2023.

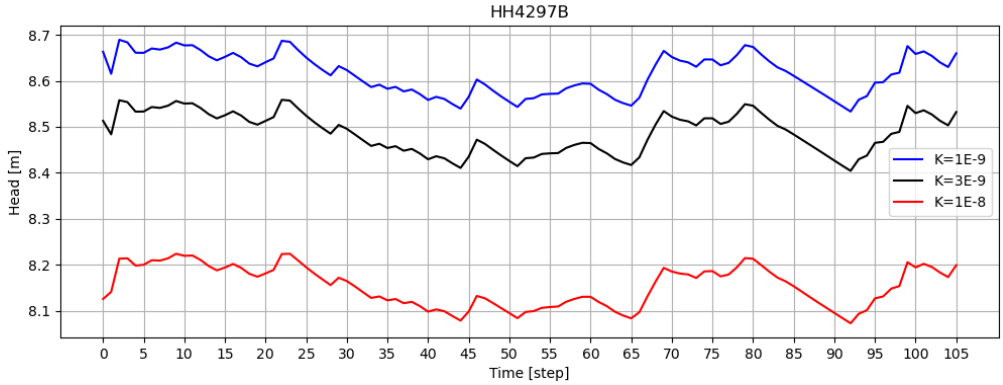

Appendix 23 Simulated head for different conductivity in the tunnel for HH4297B, 2021-2023.

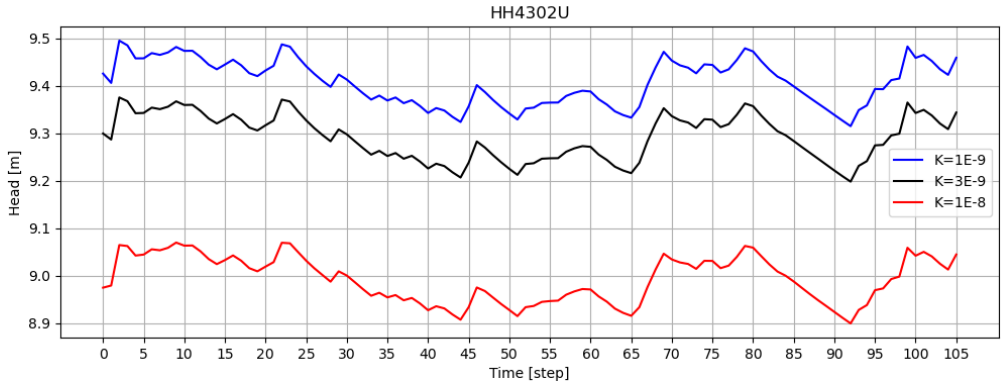

Appendix 24 Simulated head for different conductivity in the tunnel for HH4302U, 2021-2023.